REMOVAL OF MIXED VOCS OF BENZENE, TOLUENE, AND XYLENE BY USING CATALYTIC CORONA DISCHARGE SYSTEM

Issaree   Tantiprapa

A Thesis Submitted in Partial Fulfilment of the Requirements

for the Degree of Master of Science

The Petroleum and Petrochemical College, Chulalongkorn University

in Academic Partnership with

The University of Michigan, The University of Oklahoma,

Case Western Reserve University, and Institut Français du Pétrole

2018

ABSTRACT

Silver (Ag) and Manganese (Mn) catalysts were loaded on TiO_2 and Al_2O_3 supports on quartz wool that were tested for the oxidation of mixed Volatile Organic Compounds (VOCs) of benzene, toluene, and xylene in nonthermal plasma corona discharge. The total feed concentration of VOCs was fixed at 100 ppm. The catalyst located between the pin and plate electrodes with a constant gap distance of 15 mm and the pin and plate plasma reactor had an inside diameter of 9 mm. The outlet stream was analyzed by gas chromatography equipped with TCD and FID detectors. The operating parameters including applied voltage, input frequency, and types of catalysts could affect to the performance of VOCs removal process especially the selectivity for CO_2. For the sole plasma system, the optimum conditions of an applied voltage of 5 kV and an input frequency of 500 Hz provided a relatively high VOCs conversion with the highest CO_2 selectivity. Among all studied catalysts, the 4%Ag/Al_2O_3 catalyst in the pin and plate corona discharge reactor was found to improve the CO_2 selectivity from 59 to 81% while the CO selectivity was reduced from 31.3 to 6.0%. Due to the catalyst provided high surface area for oxidation reaction and also provide the metal oxide on surface which completely reacted with other hydrocarbon and CO molecules could stayed longer in plasma zone that leaded to the opportunity of CO molecules further oxidized with active oxygen in the system become CO_2.

บทคัดย่อ

อิสรีย์ ตันติประภา : การสลายตัวของสารประกอบอินทรีย์ชนิดระเหยง่าย ซึ่งประกอบด้วย
เบนซีน,โทลูอีน,และไซลีน ในเครื่องปฏิกรณ์พลาสมาแบบปล่อยโคโรน่า โดยการช่วยเหลือของตัวเร่ง
ปฏิกิริยา ที่อุณหภูมิห้องและความดันบรรยากาศ (Removal of Mixed VOCs of Benzene,
Toluene, and Xylene by using Catalytic Corona Discharge System.) อ. ที่ปรึกษา ศ. ดร.
สุเมธ ชวเดช 98 หน้า

ตัวเร่งปฏิกิริยาเงิน(Ag) และแมงกานีส(Mn) ที่อยู่บนตัวรองรับไททาเนีย(TiO_2) และอลูมินา
(Al_2O_3) บนใยควอตซ์ ในการศึกษาการออกซิเดชันของสารประกอบอินทรีย์ระเหยง่ายซึ่งประกอบไป
ด้วยเบนซีน,โทลูอีน,และไซลีน โดยกำหนดความเข้มข้นเริ่มต้นของสารประกอบอินทรีย์ระเหยง่าย ไว้
ที่100ppm ตัวเร่งปฏิกิริยาถูกจัดวางอยู่ตรงกลางระหว่างขั้วและแผ่นอิเล็กโทรดที่มีระยะห่างคงที่ 15
มม. ภายในเครื่องปฏิกรณ์แบบพลาสมามีเส้นผ่านศูนย์กลางด้านในขนาดเท่ากับ9มม. สายขาออก
จากเครื่องปฏิกรณ์ถูกวิเคราะห์โดยเครื่องแก๊สโครมาโทรกราฟีที่ติดตั้งเครื่องตรวจจับแบบTCDและ
FID ปัจจัยที่ส่งผลต่อการทำงานและประสิทธิภาพในการออกซิเดชันของสารประกอบอินทรีย์ระเหย
ง่ายอาทิเช่น แรงดันไฟฟ้า,ความถี่,และชนิดของตัวเร่งปฏิกิริยา ผลการทดลองพบว่าสภาวะที่
เหมาะสมสำหรับเครื่องปฏิกรณ์พลาสม่าแบบปล่อยโคโรนาสำหรับระบบพลาสมาเพียงอย่างเดียวคือ
แรงดันไฟฟ้าที่ 5 กิโลโวลต์ และความถี่ 500 เฮิรตซ์ ซึ่งให้ค่าการสลายสารประกอบอินทรีย์ชนิด
ระเหยง่ายในอัตราที่สูงและการค่าเลือกเกิดของแก๊สคาร์บอนไดออกไซด์สูงที่สุด การมีอยู่ของตัวเร่ง
ปฏิกิริยาในระบบจากตัวเร่งปฏิกิริยาทั้งหมดที่ศึกษาพบว่าการใช้ตัวเร่งปฏิกิริยาเงินในร้อยละ4ของ
น้ำหนักของตัวรองรับอลูมินามีส่วนช่วยในการเพิ่มค่าการเลือกเกิดแก๊สคาร์บอนไดออกไซด์ จากร้อย
ละ 59 เป็นร้อยละ 81 ในขณะเดียวกันค่าการเลือกเกิดแก๊สคาร์บอนมอนนอกไซด์ลดลงจากร้อยละ
31 เป็นร้อยละ 6 การมีอยู่ของตัวเร่งปฏิกิริยามีส่วนช่วยในการเพิ่มประสิทธิภาพการสลาย
สารประกอบอินทรีย์ระเหยง่ายเนื่องจากตัวรองรับมีค่าพื้นผิวที่มากทำให้เพิ่มโอกาสการ
เกิดปฏิกิริยาออกซิเดชันของระบบนอกจากนั้นยังมีตัวเร่งปฏิกิริยาออกไซด์อยู่บนพื้นผิวที่ทำปฏิกิริยา
โดยสมบูรณ์กับสารประกอบอินทรีย์ชนิดระเหยง่ายทำให้แก๊สคาร์บอนมอนอกไซด์เกิดปฏิกิริยา
ออกซิเดชันอีกครั้งและกลายเป็นแก๊สคาร์บอนไดออกไซด์ในที่สุด

ACKNOWLEDGEMENTS

TABLE OF CONTENTS

LIST OF TABLES

LIST OF FIGURES

CHAPTER I
INTRODUCTION

Nowadays, energy demand is gradually increasing due to the growing of economics. Air pollution is perceived as a modern-day curse: a by-product of increasing urbanization and industrialization, resulted from the increasing of automobiles around the world. In pursuit of the above, the fuel consumption rate rapidly increases which directly affect to the rise of exhaust gas emission rate. Exhaust gas normally consists of nitrogen oxides (NO_x), sulphur oxides (SO_x), hydrogen disulfide (H_2S) and mainly volatile organic compounds (VOCs).

Volatile Organic Compounds (VOCs) are organic hydrocarbons that have a high vapor pressure and low boiling point at ordinary room temperature which contribute to easily evaporate or sublimate of liquid and solid to form gas phase. (Elfadly, *et al.,* 2016). Because of its high volatility, VOCs spread in atmosphere rapidly, which have been considered as large negative impact on both environment and human health such as ozone network depletion and carcinogenic for human (Vandenbroucke, *et al.,* 2011). Begerow *et al.* (1996) investigated benzene, toluene, and xylene known as BTX, are the markers for human exposure to VOCs; therefore, the monitoring of these three compounds is necessary in order to evaluate the risk to human health.

As a result, numbers of researches have been studied the processes and technologies of both removing and controlling VOCs. Conventional processes such as adsorption, oxidation, membrane separation, and bio-reaction. However, these methods have some limitation such as high cost investment, requires high energy consumption, the limitation of area spacing, and etc.

According to high removal efficiency and low energy consumption, Non-thermal plasma (NTP) is one choice that can be used to cover those weaknesses. NTP removes VOCs by generating active species which responsible for the oxidation of VOCs molecules. These active species will collide with hydrocarbon molecules then become non-toxic VOCs such as CO_2 and CO.

In this study, corona discharge reactor was selected to remove mixed of VOCs because it can be operated under mild condition and simplicity but high efficiency. The corona reactor is efficient in producing active oxygen radicals from air, that reacts with VOCs in gas phase through oxidation reactions of hydrocarbon molecules that will converts toxic VOCs to non-toxic products such as CO_2. Even it is an efficient technique, it still provide some toxic byproducts which the majority of CO molecules. In order to overcome this problem, the plasma catalytic process has been introduced.

In this study, silver (Ag) and Manganese (Mn) catalysts loaded on TiO_2 and Al_2O_3 were used for investigate the removal of mixed VOCs on corona discharge system and also improve the CO_2 selectivity. The studied operating parameters are applied voltage and input frequency of plasma reactor.

CHAPTER II

LITERATURE REVIEW

2.1 Benzene

2.1.1 Characteristics of benzene

Benzene is an organic chemical compound with chemical formula C6H6. Six carbon atoms join together in a ring with one hydrogen atom attached on each carbon atom. As it contains only carbon and hydrogen atoms, benzene is classified as a hydrocarbon. The color of benzene is clear or a colorless liquid. It is also highly flammable and volatile liquid. Benzene is found in crude oil and as a by-product of oil-refining processes. In industry benzene is used as a solvent, chemical intermediate, and in the numerous chemicals synthetic.
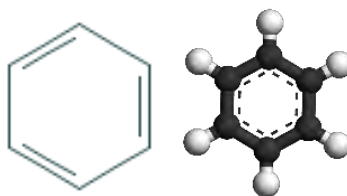
Figure 2.1 Benzene's structure.

Table 2.1 Physical properties of benzene

Chemical formula	C_6H_6
Molar mass	78.11 g·mol^{-1}
Appearance	Colorless liquid
Odor	Aromatic, gasoline-like
Density	0.8765 g/cm^3
Melting point	5.53 °C (41.95 °F; 278.68 K)
Boiling point	80.1 °C (176.2 °F; 353.2 K)
Vapor pressure	12.7 kPa (25 °C), 181 kPa (100 °C)
Viscosity	0.6076 cP (25 °C), 0.4965 cP (40 °C)

2.1.2 <u>Applications of benzene</u>

Benzene is naturally found in crude oil. Crude oil is refined into gasoline and other products by using heat, pressure and chemicals and chemical process in the refinery to separate the spectrum of petroleum products such as catalytic reforming, steam cracking toluene hydrodealkylation and toluene disproportionation. The refining process yields gasoline and a number of other petroleum products including diesel, jet fuels, solvents, lubricating oils, and many of which include small amounts of benzene.

Benzene is most commonly used as an intermediate for other chemicals such as cumene, cyclohexane, nitrobenzene, alkylbenzene, and mainly ethylbenzene in the industrial production of other chemicals because it can be used. Ethylbenzene production is the main product from benzene because it is precursor for styrene which is used for polystyrene production. Another 20% is for cumene production which is phenol intermediate. Furthermore, it can be used directly as solvent and gasoline additive.

Benzene also important in many paint products production., such as top coats, sealants, solvents, spray paints lacquers, and more. Auto repair facilities products are also produced from benzene to clean brakes, hydraulic systems, and fuel system components. It is also used in the tires rubber production and is a component of asphalt and crude oil, as well as all lubricants made from crude oil. Furthermore, benzene is often used in the production of pesticides.

For consumer products where benzene is used as a building block or intermediate, benzene is typically fully reacted in a closed system, with little to no benzene remaining in the finished consumer product.

2.1.3 <u>Benzene toxicity</u>

Benzene is highly toxic and can be considered as carcinogen; exposure to it may cause leukemia. As a result, there are strict controls on benzene emissions. There are three main factors that need to be concerned before people will harm by benzene which are dosage of benzene, duration time contract, and how benzene contract with body. Concentration of benzene in air is 0.02-0.34 ppb (part in billion parts of air). People will smell the scent when the concentration is approximately 60 ppm.

There are many ways for benzene to enter in the body such as inhalation, gastrointestinal tract and also directly through skin. After get into body, it will spread through blood system then temporarily stores in bone marrow and fat. Many governments have developed the regulations and recommendations to protect public health and they are enforced by law. The Environmental Protection Agency (EPA), the Occupational Safety and Health Administration (OSHA) and the Food and Drug Administration (FDA) are example of agencies that develop the regulations for toxic substances. Recommendations and regulations are expressed as "not-to-exceed" level. For benzene, EPA has set the maximum limit at 5 ppb and they found that 10 ppb of benzene in air can cause of cancer in human. Furthermore, the maximum for short term exposed (less than 10 days) is 200 ppb for children.

2.2 Toluene

2.2.1 <u>Characteristics of toluene</u>

Toluene occurs naturally at low levels from crude oil and is usually produced in the processes of gasoline via a catalytic reformer, in an ethylene cracker or making coke from coal. Toluene is an aromatic hydrocarbon. It is a colorless, water-insoluble liquid with the smell associated with paint thinners. It is a mono-substituted benzene derivative, consisting of methyl group ($-CH_3$) attached to a phenyl group.

Methylbenzene is called by IUPAC name. It is used as predominately of a solvent and industrial feedstock.
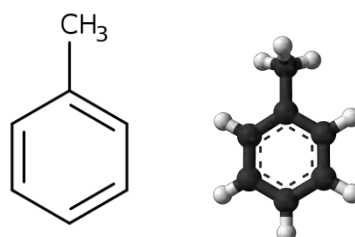
Figure 2.2 Toluene's structure.

Table 2.2 Physical properties of toluene

Chemical formula	C_7H_8
Molar mass	92.14 g·mol^{-1}
Appearance	Colorless liquid
Odor	Sweet, Pungent, Benzene-like
Density	0.87 g/cm^3 (20 °C)
Melting point	-95 °C (-139 °F; 178 K)
Boiling point	111 °C (232 °F; 384 K)
Vapor pressure	2.8 kPa (20 °C)
Viscosity	0.590 cP (20 °C)

2.2.2 <u>Applications of toluene</u>

Toluene has numerous commercial and industrial applications such as a solvent in paints, lacquers, thinners, glues, correction fluid and nail polish remover, and it is also used in the printing and leather tanning processes. Methylbenzene can also be used as a fullerene indicator, and raw material for toluene di-isocyanate. In

addition, toluene can be used as an octane booster in gasoline fuels used in internal combustion engines. Absolute toluene can be used as a fuel for both two-stroke and four-stroke engines.

2.2.3 Toluene toxicity

Toluene is lipid soluble, it has a moderate tendency to bioaccumulate in the food chain. It can release into the atmosphere, water, and soil at places where it is produced or used. Toluene is commonly found in air, particularly when there is heavy traffic or near gasoline filling station.

Principal sources of toluene indoors can be found in common household products such as paints, paint thinners, vanishes, rust inhibitors, adhesive product, sanitizing agents, and cigarette smoke. In addition, toluene is used as a solvent for cosmetic nail polished at concentration up to 50%.

Concentration of toluene for indoor air is often several times higher than outside. The systemic harmful effects can occur. It may cause irritation of the eyes, respiratory tract, and skin. Repeated or prolonged contact with the liquid may cause removal of natural lipids from the skin resulting in dry, fissured dermatitis. Low-level, chronic exposure as well as acute exposure to toluene may result in central nervous system depression and decreased memory. Other symptoms include headache, dizziness, fatigue, muscular weakness, drowsiness, and incoordination with staggering gait, skin paresthesia, collapse, and coma.

2.3 Xylene

2.3.1 Characteristic of xylene

Xylene or dimethylbenzene, the molecule composed of one benzene ring in the center which has two methyl groups attached at the substituents. Due to six carbon atoms in benzene ring, two methyl groups can attached in different ways that

cause three isomers occur which are ortho-xylene, meta-xylene, and para-xylene. Name of those mentioned isomers are related to the position that methyl groups attached. All of them are colorless, flammable liquids, some of them are great industrial value. The chemical formula of xylene is (CH3)2C6H4 for all isomers. Xylene is both naturally occurring and manmade, and is widely used as a solvent in the leather, rubber and printing industries. Other applications of xylene include chemical intermediates, and high-motor and aviation gasoline blending agents.

1,2-dimethylbenzene   1,3-dimethylbenzene   1,4-dimethylbenzene
(*ortho*-xylene)   (*meta*-xylene)   (*para*-xylene)
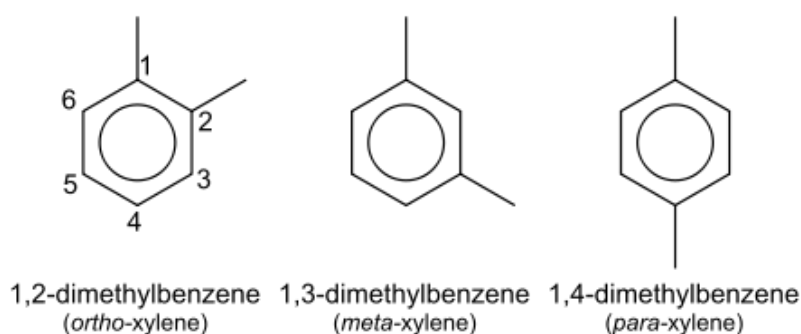
Figure 2.3 Xylene's structure.

Table 2.3 Physical properties of xylene

Properties	Isomer		
	Ortho-Xylene	Meta-Xylene	Para-Xylene
Chemical formula	C_8H_{10}		
Molar mass	106.16 g/mol.		
Appearance	Clear and Colorless liquid		
Odor	Sweet		
Density	0.88 g/mL, liquid	0.86 g/mL, liquid	0.86 g/mL, liquid
Melting point	-25 °C (-13 °F; 248 K)	-48 °C (-54 °F; 225 K)	13 °C (55 °F; 286 K)
Boiling point	144 °C (291 °F; 417 K)	139 °C (282 °F; 412 K)	138 °C (280 °F; 411K)
Vapor pressure	2.4 kPa (37.7 ° C)		
Viscosity	0.812 cP at 20 °C	0.62 cP at 20 °C	0.34 cP at 30 °C

2.3.2 Applications of xylene

The production of xylene is occurred from crude oil pass through the process called alkylation. The color is clear, colorless liquid also has a sweet-smelling solution. The ratio of xylene isomers can be shifted to favor the highly-valued which is para-xylene via the patented UOP-Isomar process or by trans alkylation of xylene with itself or tri-methylbenzene. These conversions are catalyzed by zeolites. ZSM-5 is used to facilitate some isomerization reactions leading to mass production of modern plastics.

In common uses, xylene is a raw material in the monomer (a simple compound with molecules that join together to form polymers) production called terephthalic acid which has been used in the manufacture of polymers and it is a basic petrochemical used in the textile industry for making polyester. Para-xylene is a very important raw material in the preparation of PET (polyethylene terephthalate) chips, which are extensively used in packing industries; mineral water and carbonated soft drink bottles. It is a good cleaning agent for silicon wafers and steel. It is also used to sterilize many substances. Xylene is used as a feedstock in the petrol production. It is also found in small proportions in gasoline and jet fuel. Moreover, mixed xylene can be used in printing industries, pharmaceuticals, perfumes, fabricated items and some pesticides formulation.

2.3.3 Xylene toxicity

Main sources of xylene emission are industrial factories, automobile exhausted gas, and laboratories in form of solvents. Xylene is rapidly absorbed after inhalation through lungs which is the most common route exposure of xylene. Xylene's odor threshold is about 1 ppm which lower than OSHA's limitation (100 ppm.) that adequate for warning in hazardous. When the concentration is about 200 ppm. can cause eyes and throat irritation. The xylene vapor is heavier than air then may cause asphyxiation in enclosed, poorly ventilated, or low-lying areas.

Furthermore, xylene can directly contact through skin and eyes. Its vapor is only mildly irritating to mucous membranes. However, xylene splashed in the eyes can result in corneal injury. Repeated or prolonged skin contact with liquid xylene can defat the skin causing it to crack and peel. Percutaneous absorption is slow through intact skin; however, xylene absorbed through the skin may contribute to body burden.

2.4 Volatile organic compounds (VOCs)

Volatile organic compounds (VOCs) are organic chemicals hydrocarbon that have a high vapor pressure at ordinary room temperature. The high vapor pressure due to low boiling point which results in molecules can easily evaporate or sublimate from liquid and solid to become gas phase. Mostly VOCs are considered to hazardous pollutants that emitted from automobile exhausted, paints, solvents, industrial facilities and etc. Some VOCs are harm to human health, as a carcinogen, and environment. Recently, VOCs are also recognized as causative agent of sick building syndrome. In addition, the emission of VOCs can cause various effects such as photochemical smog, the formation of ozone, stratospheric depletion, and intensification of global warming.

2.4.1 Exposure situation of VOCs

There is some evidence on animal studies indicated that some of these VOCs have carcinogenic or mutagenic effects on tissue development. Benzene is one of these chemicals which are classified by US EPA as a human carcinogenic compound group A (EPA1, 2005). Begegrow *et al*. (1996) investigated benzene, toluene, and xylene that known as BTX, they are the markers for human exposure to VOCs; therefore, the monitoring of these three compounds is necessary in order to evaluate the risk to human health.

The research of Ongwandee *et al*. (2010) investigated VOCs concentrations in four public transportation modes in Bangkok, Thailand during two rush hour periods which are in the morning that most people are going to work and

evening when they come back home (7:00 -9:00 a.m. and 4:00 – 6:00 p.m.). Types of transportation included an air-conditioned bus (A/C bus), non-air-conditioned bus (non-A/C bus), electric sky train (BTS), and a boat traveling along the canal. The studied locations were the three main important roads. Charcoal sorbent tubes were used for collecting in-vehicle air samples then analyzed by a gas chromatography-mass spectrometer (GC-MS). Results showed that the transportation modes significantly influenced the abundance of in-vehicle benzene, toluene, ethylbenzene, and meta, para-xylene (BTEX). Median concentrations of BTEX were 11.7, 103, 11.7, and 42.8 µg/m3 in A/C bus; 37.1, 174, 14.7, and 55.4 µg/m3 in non-A/C bus; 2.0, 36.9, 0.5, and 0.5 µg/m3 in sky train; and 3.1, 58.5, 0.5, and 6.2 µg/m3 in boat, respectively. Wilcoxon rank sum test indicated that toluene and meta, para-xylene in the sky trains were statistically lower than that in the other three types of transportation at a p-value of 0.05. There were statistical differences in TEX concentrations among the bus routes in the non-A/C buses. In addition, the benzene to toluene ratios implied that tail-pipe emissions were important contributor to the abundance of in-vehicle VOCs. The results showed significantly higher levels of BTEX in both A/C and non-A/C buses than in sky trains or passenger boats. The air inside sky trains had significantly low concentrations of toluene and meta, para-xylene. Comparison among metropolitan cities revealed that Bangkok bus commuters are exposed to the high levels of BTEX compounds. This may be due to the high aromatic content fuel and severe traffic congestion.

In addition, the research of Kanjanasiranont *et al*. (2017) also confirmed the effect of severe traffic congestion to high exposed of VOCs in air especially benzene, toluene, ethylbenzene, and xylene. The studied location were in the severe traffic congestion which are on Pathumwan intersection (PT), Chaloem Pao junction (CP), Sam Yan intersection (SY) and Henry Dunant intersection (HD). The highest concentration of BTEX was detected at HD (range from 1,570.46 to 5,553.77 µg/m3, average 2,968.96 µg/m3) and the lowest at SY (range from 1,179.99 to 2,859.31 µg/m3, average 1,964.52 µg/m3). Moreover, the researchers studied the effect of carbonyl compounds (CCs) which are also toxic air pollutants including carcinogenic compounds that have high potential to cause health problems. For CCs compounds,

formaldehyde and acetaldehyde were found at the most abundant in CCs. Similar to BTEX, the highest average concentrations of both formaldehyde and acetaldehyde were detected at HD (range from 13.76 to 32.42 µg/m3, average, 21.50 µg/m3, and range from 3.90 to 99.70 µg/m3, average, 64.82 µg/m3, respectively). In conclusion, high traffic density leads to higher levels of air pollution and roadside workers who are exposed to these pollutants everyday are therefore at risk.

2.4.2 VOCs emission control

According to the previous researched, there is high concentration of VOCs in air that will be the pollutants. Controlling and treating of VOCs are become important issues. The removal methods of VOCs from polluted air are listed by the following (Urashima & Chang, 2000).

2.4.2.1 Conventional methods

Solvent recovery adsorption is defined as the concentration of a substance (adsorbate) would be adsorbed into the surface of a solid (adsorbent). The basic principle of adsorption is applied to air emission control when a solvent laden air stream passes through a bed of high-surface-area solids material (typically carbon, alumina, silica gel or molecular sieve). These materials will capture the substance into their surfaces. This technique can remove VOCs with 95 - 98 % efficiency but requires high investment and maintenance cost.

Thermal Oxidation, this method is widely used in petrochemical industries. Thermal oxidizers are typically used to convert hydrocarbon molecules into carbon dioxide (CO_2) and water (H_2O) through oxidation reaction. This process is carried out by raising the temperature of the process exhaust gas stream to break the hydrogen-carbon bonds approximately 760 - 780 °C with the maximum residence time of 1 second providing new bonds to form, creating CO_2 and H_2O. This reaction is exothermic reaction, heat is released. The limitation of this technique is VOCs concentration need to be high in order to be used as fuel. Nitrogen oxides (NO_x) (products of combustion) increase as temperature and fuel inputs increase. NO_x output

should be also considered because it is a primary component in the production of ozone.

Condensation and gas absorption are most commonly used for highly concentrated VOC streams that are advantageous to recover and the relatively large expense is warranted. It employs a drop in temperature and/or increase in pressure. The cleaned air stream is separated from the condensate containing target pollutants. In many cases, very large temperature drops are required to achieve effective condensation and requiring significant energy investment to accomplish cooling.

Moreover, there are many conventional methods to control amount of VOCs in air such as membrane separation, bio-reaction, catalytic and thermal oxidation. By the way, those mentioned methods have a lot of disadvantages such as system efficiency, operation hardness and cost efficiency (Vandenbroucke, *et al*., 2009).

2.5 Plasma

Plasmas are a source of gas-phase free radicals and other active species which are useful for destroying pollutants. Reactive species in non-thermal plasma can react with odorous, toxic gases and vapors then convert them into non-odorous and non-toxic molecules. The increasing in temperature, molecules change into have more energetic and transform matter by the sequence: solid, liquid, gas and finally plasma that is thus considered the fourth state of matter.

2.5.1 Definition of plasma

The concept of plasma originates from the fundamental difference between regions of electrical gas discharges. It could be partially or fully-ionized gas which is roughly zero charge (positive and negative charge are unbounded). When a neutral gas is ionized, it behaves as a conductive media. Ionization process is the

phenomenon creating the pair of negatively and positively charged particles (Keidar & Beilis, 2013). The positive charge particles are cations while the negative charge particle can be either electron or anions. Even these particles are unbound with each other, they are not completely "free" which means it can moves freely under electric field. Moving charged particles generate an electric current within a magnetic field; and any movement of a charged plasma particle affects and is affected by the general field created by the motion of other charges. In turn, this governs collective behavior with many degrees of variation (Dendy, *et al*., 1990).

2.5.2 Generation of plasma

There are several methods for plasma generation such as combustion, electrical heated furnaces and electrical discharge (glow, arc microwave, corona, and etc.) that depends on energy level, temperature, and ionic density. Plasma is generated by applying electric across the metal electrodes to electrical discharge system. The metal electrodes generate free electrons which are accelerated in the electric field until energy is sufficiently supplied. It will produce electron and ions in gas phase to cause ionization through collision with molecule of feed. There are various methods for supplying energy to neutral gas to form plasma. Generally there are two types of plasma recognized, thermal and non-thermal plasma.

Thermal energy is one of methods for supplying energy. Exothermic reaction of molecules is used as prime energy source. Then, adiabatic compression of gas will be used for supplying energy to gas until energy level reach to plasma generation point. Energetic beams can also be used for plasma energy source. Beams of neutral particles have added advantage of being stable in electric and magnetic fields (Conrads & Schmidt, 2000).

Non-thermal plasmas are generated by applying an electric field to a neutral gas. Electrons and ions can be found at any volume of neutral gas and those free charge carriers are accelerated by the applied electric field and new charge particles are created by colliding between free charge carriers and atoms or molecules in neutral gas. Due to their light mass, electrons are selectively accelerated by the field

and gain high temperatures while the heavier ions remain relatively cold through energy exchange by collisions with the background gas. Furthermore, new charge particles can be generated by colliding between free charge carriers and surface of electrodes. These phenomena lead to avalanche of charge particles formation and they are balanced by charge carrier losses.

2.5.3 Collision process in plasma

Collision processes are categorized into 2 collision types which are elastic collision and inelastic collision. The collision will occur when electrons have gained energy in a plasma collide with atoms and molecules. Elastic collision is the collision that the kinetic energy changes while internal energy remains the same. This type of collision occurs when the energy of electron is low. The energy inside electron will transfer to kinetic energy causing the velocity which losses in small amount energy through the collision. On the other hand, inelastic collision such as ionization and excitation, the internal energy is converted these include dissociation, dissociative recombination, process involving negative ions, such as electron attachment, detachment, and positive-negative ion charge transfer, and process involving excitation of molecule vibrations and rotations.
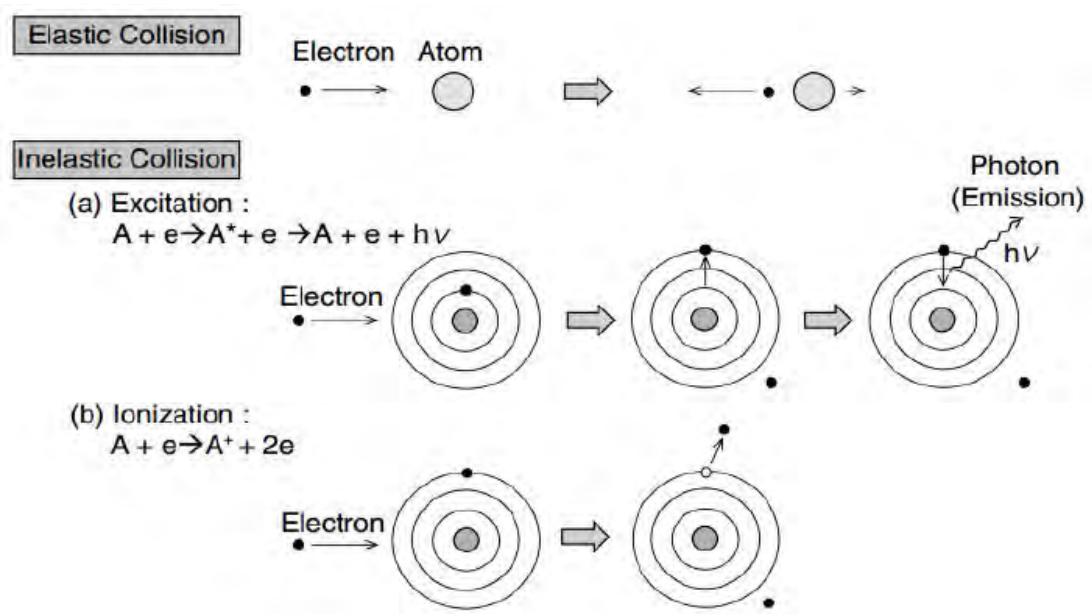
Figure 2.5 Summarizes the collision process in plasma.

2.5.3.1 Excitation

A state of system that has higher energy than ground state, after electron colliding with atom, it provides the energy to the electron inside atom bounces to the higher energy level, causing of unstable situation. After bounced out, it will emit the photon during the transition then bounce back to ground state. An excitation state is represent as follows ;

$$A + e \longrightarrow A^* + e \longrightarrow A + e + h\nu$$
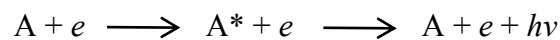
Where A is neutral atom, A* is A in excited state, h is Planck's constant, ν is the frequency of emitted photon.

2.5.3.2 Ionization

After colliding, the outermost shell electron is expelled when the energy of ionization voltage is smaller than colliding with free electron that cause a neutral atom turns to be positive ion which is described as follows ;

$$A + e \longrightarrow A^+ + 2e$$
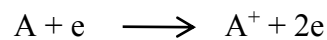
2.5.3.3 Dissociation

Dissociation is the state that atom split or separate into smaller molecule or atom. This occurred when the free electron colliding energy is higher than binding energy between atom or molecule which described as follows ;

$$AB + e \longrightarrow A + B + e$$
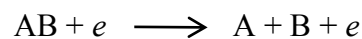
2.5.3.4 Electron attachment

After colliding with free electron, the atom turns into negative ion which described as follows ;

$$A + e \longrightarrow A^-$$
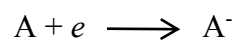
2.5.4 <u>Classification of plasma</u>

Based on their energy level, temperature, and electron density. It can be classified into two main categories in chemical applications which are high temperature and low temperature plasma as shown in Table 2.5. High temperature plasma is implied that electrons, ions and neutral species are in a thermal equilibrium states. Low temperature plasma is further subdivided into thermal plasma (quasi-equilibrium plasma) and non-thermal plasma (non-equilibrium plasma or cold plasma).

For high temperature plasma, equilibrium state will occur at the temperature range of 10^5-10^7 K when the temperature of gas (T_0) is closed to the electron temperature (T_e), the number of collisions electron increases resulting in dispersing energy. The examples of thermal plasmas are arcs and plasma torches which are used for the work that requires high temperature such as spraying or Inductive Coupled Plasma (ICP) for analyzing element in sample which is greater than Atomic Absorption Spectroscopy (AAS).

For low temperature plasma, it will occur at temperature of gas is much lower than the temperature of electron ($T_0 \ll T_e$). For examples, plasma generated by glow discharge occurs at lower pressure about 1 kPa and $T_e \sim 10,000$ K. The temperature of neutral species does not change whereas the temperature of electrons is very high. Obviously that plasma is not play important role to provide energy to the system; nonetheless, generate exciting species and radicals allowing initiating and enhancing the chemical reactions.

Therefore, non-thermal plasma is often used for activating chemical reactions which occur at lower temperature than needed while high temperature plasma requires electrical energy for heat gas. The non-thermal plasma is related to low temperature or another word lower the energy consumption which is one of non-thermal plasma advantages (Paulmier & Fulcheri, Use of non-thermal plasma for hydrocarbon reforming, 2005).

Table 2.4 Classification of plasma (Hippler, *et al.,* 2007)

Low temperature plasma (LTP)		High temperature plasma (HTP)
Thermal LTP	Non-thermal LTP	$T_i \approx T_e \geq 10^7$ K
$T_o \approx T_e \approx T \leq 2\times10^4$ K	$T_o \approx T \leq 300$ K	$n_e \geq 10^{10}$ m^{-3}
$n_e \geq 10^{20}$ m^{-3}	$T_o \ll T_e \leq 10^5$ K	e.g., fusion plasma
e.g., arc plasma at normal pressure	$n_e \geq 10^{20}$ m^{-3}	
	e.g., low-pressure glow discharge	

2.5.5 Type of Non-thermal Plasma

Non-equilibrium plasma can be classified into several types depending on their generation mechanism, pressure range, and the electrode (Eliasson, *et al.*, 1987).

2.5.5.1 Glow Discharge

The glow discharge, or low pressure discharge is typically produced in a low-pressure than 10 mbar. It is produced by two metal electrodes surrounded by a low-pressure gas which enclosed in a glass tube that contains a low-pressure gas. The ionized gas become a plasma which conducing electricity, after higher voltage reached. This type of discharge is usable in neon and fluorescent tubes but not for chemical synthesis due to its low pressure and mass flow thus it is not suitable for chemical synthesis in the industry.

2.5.5.2 Dielectric Barrier Discharge (DBD)

Dielectric barrier discharges (silent discharges) are used on a large industrial scale. They combine the advantages of non-equilibrium plasma properties with the ease of atmospheric-pressure operation. A prominent feature is the

simple scalability from small laboratory reactors to large industrial installations with megawatt input powers.

Figure 2.6 Schematic of dielectric barrier discharge ; (1) metallic electrodes and (2) dielectric barrier coating.

The specific DBD configuration used for plasma actuators consists of two electrodes, one uncoated and exposed to the air and the other encapsulated by a dielectric material (Figure 2.6). As a consequence of the presence of at least one dielectric barrier (e.g. glass, quartz, ceramic, and etc.) these discharges require alternating voltage for their operation. The dielectric, being an insulator, cannot pass a DC current. For plasma actuator applications, the electrodes are arranged in a highly asymmetric geometry as opposed to the parallel-plate arrangement that requires properly certain location in the discharge gap between to electrodes and sufficiently voltage that high enough to ionise the gas, which spreads out from the edge of the exposed electrode to the side under which the lower electrode is placed. The discharge is self-limiting, whereby charge emitted from the exposed electrodes gradually accumulates on the dielectric surface and reduces the potential difference. This type of plasma has been known for more than a century, Kogelschatz, et al., (2003) has been used DBDs in the industrial applications for ozone generation and pollution control. The configuration of DBD is shown in Figure 2.7.
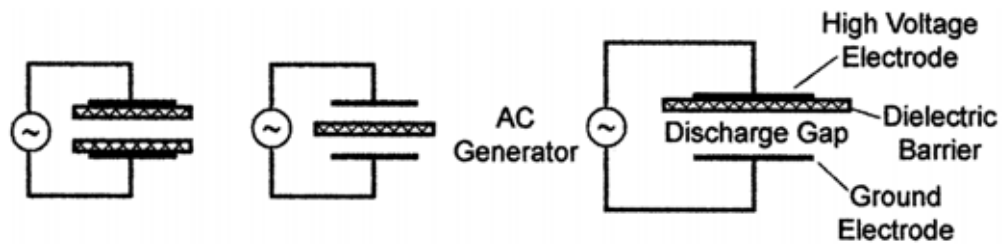
Figure 2.7 Basic dielectric-barrier discharge configurations.

After the ignition of the discharge, charged particles are collected on the surface of the dielectric. This charges build-up create a voltage drop, which counteracts the applied voltage, and therefore chokes the discharge current. The discharge subsequently extinguishes. As the applied voltage increases again (at the second half cycle of the applied voltage) the discharge reignites. This process is repeated over and over during each full cycle of the applied voltage.

At very high frequency the current limitation by the dielectric becomes less effective. For this reason, DBDs are normally operated between line frequency and about 10 MHz The gap is on the order of several mm, and the applied voltage is about 20 kV. When the electric field in the discharge gap is high enough to cause breakdown, in most gases many micro discharges are observed when the pressure is of the order of 105 Pa. This is a preferred pressure range for ozone generation, excimer formation, as well as for flue gas treatment and pollution control.

In this filamentary mode plasma formation resulting in electrical conductivity are restricted to the micro discharges. The gas in between is not ionized and serves as a background reservoir to absorb the energy dissipated in the micro discharges and to collect and transport the long-lived species created. In most high-power applications, liquid cooling of at least one of the electrodes is used.

DBD is a typical non-equilibrium high-pressure AC gas discharge. Recently, two types of DBD arrangements are developed; volume discharge VD and surface discharge SD. Both are beneficial for industrial because they can be operated both in atmospheric and vacuum condition. Furthermore, DBD can generate the high energetic and high-density electron which in the range of 1-10 eV. Its unique

advantageous are to generate low excited atomic and molecular species, free radicals and excimers with several electron volts energy. Due to its attractive characteristics, DBD is recently widely studied for potential industrial applications. Ozone generators, excimer radiation sources, free radical generation and their applications in pollution control and monitor (Xu, *et al.*, 2001).

2.5.5.3 Corona Discharge

A corona discharge appears as a luminous glow localized in space around a point tip in a highly nonuniform electric field. This plasma type is generated at atmospheric pressure when sharp points, edges, or thin wires are subjected to a large sufficiently electric field with low electrical energy consumption. Corona is named from "crown" by mariner's observation of discharge on their ship mast during electrical storms.

The corona discharge is often DC-driven discharge in which many streamers are initiated from one electrode and may or may not reach the other electrode due to the conditions. DC corona discharge can be classified in many forms based on the configuration of electrode and field polarity. (Chang, et al., 1991) Point-plane or pin-plate is the most popular configuration of positive corona discharge that has a needle electrode placed above the plane electrode as shown in Figure 2.8.
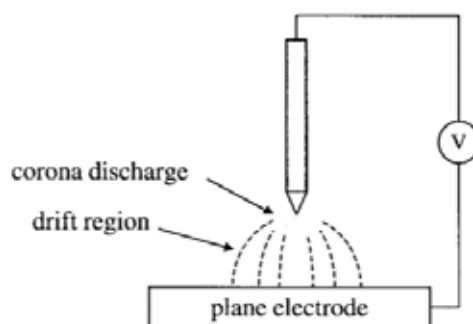
Figure 2.8 Schematic of corona discharge.

For positive corona discharge in pin-plate configuration, after applied voltage to the system the discharges start with burst the pulse corona then proceed to the streamer corona, glow corona, and then spark discharge as the applied voltage increasing. For negative corona in the same geometry configuration, Trichel pulse is an initial form of corona followed by pulseless corona and the spark discharge occurs as the applied voltage increasing as shown in Figure 2.9

(a)   (b)

Trichel   Pulseless   Spark   Burst   Streamer   Glow   Spark
Pulse   Corona   Pulse   Corona   Corona
Corona   Corona
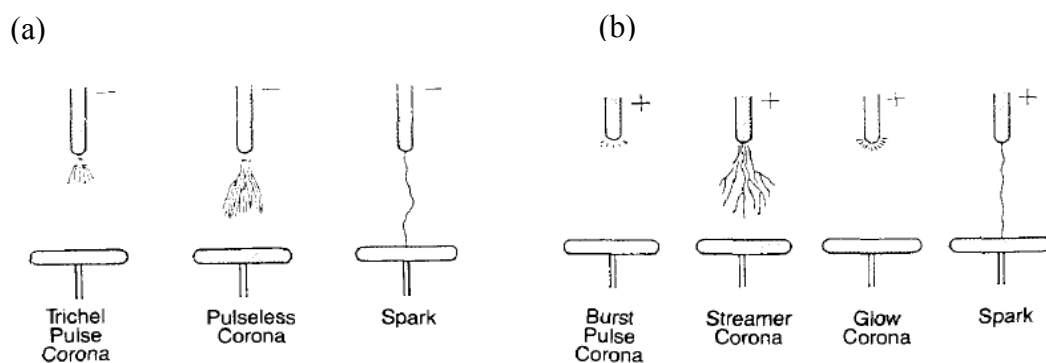
Figure 2.9 Schematic of two types of point-plane corona discharge ; (a) negative discharge and (b) positive discharge.

Negative corona discharge generally propagates by impact ionization of the gas molecules. Positive corona discharge depends more on photo-ionization for its propagation: the positive streamer, for example, may advance at as much as one percent of the speed of light. In either case, the ultraviolet photon flux from ion-electron re-combinations is quite large.

The positive corona is characterized by a steady current at a fixed voltage, quiet operation, and almost no sparking. The positive streamer corona is a discharge confined to a narrow channel which originates at the electrodes. It produces an unsteady current (because the streamer is repetitive), is quite noisy, and is the direct precursor to a spark: once streamers form at an electrode, the sparking potential has almost been reached.

The negative glow usually requires clean, smooth electrodes for generation. The glow is made up of individual electron avalanches which trigger successive avalanches at nearby locations. The total current from the electrode is relatively steady, but it is composed of many tiny pulses. The discharge is noisy and the sparking potential is high when compared with the positive streamer corona. The glow often changes with time into the tuft form, a process associated with the formation of more efficient mechanisms of generating successive avalanches. The tuft corona is also noisy and has a similar sparking potential to the glow form. The average current is steady, but it composed of tiny pulses like the glow corona. The tuft corona is more spatially in homogeneous than the glow corona. Differences between negative tuft and glow coronas have been investigated recently.

2.6 Catalytic Plasma reactors

The application of plasma techniques in the preparation of catalysts and in catalytic reactions were published during the last fifteen years were briefly reviewed. The efficiency of NTP reaction has been addressed based on reducing the power consumption and suppressing the undesired by-product formation. A variety of corona discharge reactors have been used for the destruction of various VOCs, however, the desired total oxidation to CO_2 was not achieved. In addition, formation of toxic by-products like CO, NOx was observed.

2.6.1 Configuration of catalyst in the reactor

To overcome those limitations, catalytic plasma technique has been proposed, where the catalyst is placed either in the discharge zone (in-plasma catalytic reactor) or after the discharge zone (post-plasma catalytic reactor) (Subrahmanyam, *et al.*, 2007).

2.6.1.1 In-plasma catalytic reactor (IPC)

For IPC, the plasma and catalyst regions are either completely or partially overlap. Plasma discharges are ignited within the catalyst bed or on electrodes that are coated with catalysts. An overlap between plasma and catalyst makes a strong interaction which can affect their properties. For the effect of plasma on the catalyst, the catalyst directly contacts with the discharge and the active species are generally short-lived species such as excited-state atoms and molecules, reactive radicals, photons, and electrons. In addition, the plasma may be prepared or modify the catalyst surface during the process by plasma-induced surface heating. For the effect of catalyst on plasma, catalyst also increases the lifetime of active species by the absorption process (Durme, *et al.*, 2008).

2.6.1.2 Post-plasma catalytic reactor (PPC)

For PPC, catalyst will be separated that plasma will be setup either upstream or downstream of the catalyst. For upstream-placed plasma, the plasma role is to provide reactive chemical species for being easier converted so that the catalyst is exposed only to species that exit from the plasma region or long-lived species. For downstream-placed plasma, the role of plasma is to convert the residual reactants and destroy the undesired byproducts generated from thermal catalysis (Chen, *et al.*, 2008)

(a)   (b)
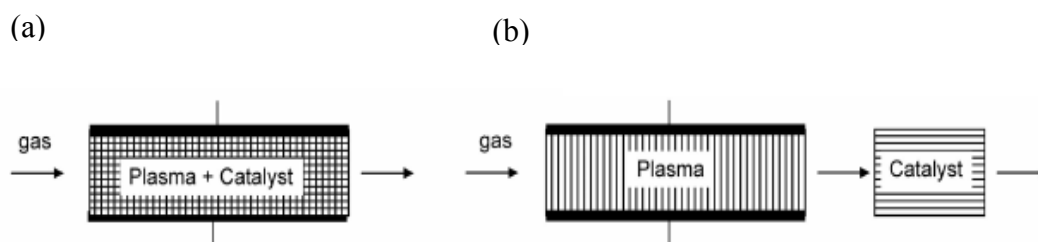
Figure 2.10 Schematic of (a) in-plasma catalysis (IPC) and (b) post-plasma catalysis (PPC).

2.6.2 <u>Metallic catalysts</u>

The development of noble metal catalysts and transition metal oxides for catalytic oxidation of VOCs has been widely reported in the literature (Liotta, 2010). There have been a number of reports on catalytic oxidation of VOCs on transition metal oxides.

2.6.2.1 Silver (Ag)

Silver is the most widely applied for the selective oxidation of ethylene to ethylene oxide with minimal production of carbon dioxide and water as by-products. Silver catalysts were found to be slightly more selective toward the formation of CO_2 when compared with other metal catalysts. The adsorption of oxygen on silver would perhaps most important and certainly the most controversial; it has received by far the most extensive treatment in the literature. Aside from insight into the role of oxygen in the initiation of stated reactions, the adsorptive characteristics of oxygen on silver also would provide a means of obtaining the free metallic surface area of silver on supported silver catalysts through selective chemisorption

2.6.2.2 Manganese (Mn)

Manganese (Mn) provide ability to adsorb $HO^{\bullet}$ radical on their surfaces in plasma reaction which could enhanced the toluene decomposition efficiency. MnO_x also enhanced the CO_2 selectivity due to that active oxygen species formation through the decomposition of O_3 on surface of catalyst. Active oxygen would further oxidize CO and toluene into CO_2. Therefore a higher CO_2 selectivity was achieved (Chavadej, *et al.,* 2007). When compared with other metal oxide, MnO_x shows a much larger BET surface area. Indicating higher dispersion of catalysts and larger contact area between active component and gas leading to better catalytic activity (Guo, *et al.,* 2010).

2.6.3 <u>Support catalyst materials</u>

Non-thermal plasma is widely used for the modification of surface oxides and for the preparation and regeneration of catalysts as well as for catalytic synthesis and decomposition. The surface of a catalyst takes a particular place among the surfaces with specific requirements. For reasons of economy and environmental concern, catalytic processes require continuous improvements. Such improvements may be achieved by different ways. One way is to find out new modes for the preparation of catalytic materials that promote the desired reactions (Kizling, *et al.*, 1996).

Many catalysts have been tested for enhancing the decomposition of VOCs, minimization of CO selectivity, and CO_2 selectivity improvement. Metal oxides are usually employed as a support for metal catalysts. It is well known that the adhesion and interaction between the metal particles and the support are important factors that influence the stability, activity and selectivity of a catalyst. Techniques of surface modification, for example plasma, can be used in order to improve the adhesion or to modify interaction between metal and support.

2.6.3.1 Titanium dioxide (TiO_2).

Titanium dioxide (TiO_2) is the one of catalyst that provide a good physical properties which is high surface area providing the stable catalysts in their mesoporous structure. In addition, TiO_2 supported metal catalyst is very attractive as its high activity for the decomposition of a wide range of VOCs (Parvulescu, *et al.,* 2012). Lee *et al*. (2004) found that TiO_2 is less toxic powder, efficient to increase the benzene conversion, and CO_2 selectivity. In addition, another researcher; Li *et al*. (2002) reported that TiO_2 also improved the toluene decomposition. When compare with the effect of metal trace loading on TiO_2, Ag/TiO_2 provides the best performance of enhancement CO_2 selectivity.

2.6.3.2 Alumina (Al$_2$O$_3$).

Alumina; aluminium oxide (Al$_2$O$_3$) is another interesting material due to its high catalytic activity that utilizes O$_3$. Porous Al$_2$O$_3$ pellets were expected to act as an adsorption material to dilute the concentration of benzene in the reactor. In particular, Al$_2$O$_3$ is known to possess electron-accepting acidic centers of various strengths that adsorb organic compounds with electron systems (Ogata, *et al.*, 1999). Sano *et al.* (2006) perform an experiment by dope trace metal on Al$_2$O$_3$ and investigated the effect of catalyst in plasma. The γ-Al$_2$O$_3$ reduced some of byproducts that generated by NTP process without obstruct the decomposition of VOCs. (Song, *et al.,* 2002).

2.7 Literature Review

Based on plasma, there is more recently technology that has become significant due to its advantages such as low costs, high treatment and energy efficiencies, smaller volume required, etc. In order to commercialize this new technology, the treatment rate, energy efficiency of treatment, pressure drop of reactor and reusable by-products production rate must be improved based on the identification of major fundamental mechanism of processes, optimization of reactor and power supply for integrated system (Jen-Shih Chang, 2001).

Ogata, et al., (2000) have studied the effect of water vapor on benzene decomposition using a non-thermal discharge plasma reactor. In order to clarify the effect of H$_2$O addition, the decomposition of benzene was investigated in air, in humidified air, in N$_2$, and in humidified N$_2$. As shown in Figure 2.11, for the same input power, the energy efficiency of the reaction decreased in the following order ; air , N$_2$, humidified air , and humidified N$_2$. Thus, the efficiency was decreased by the presence of H$_2$O, irrespective of background gases. Furthermore, since the efficiency in air was higher than in N$_2$, direct electron impact as well as activated oxygen species play an important role in the initial stage of benzene decomposition.
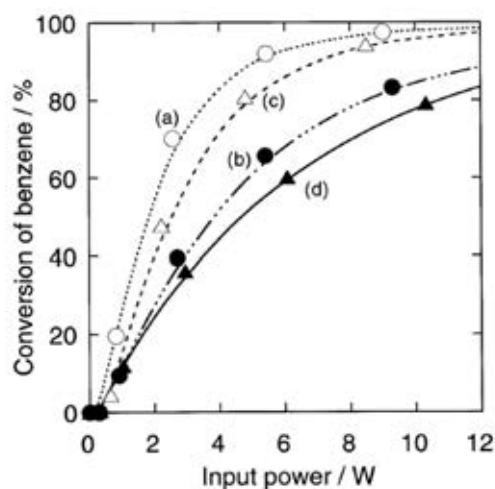
Figure 2.11 The decomposition of benzene (a) in air, (b) in humidified air, (c) in N_2, and (d) in humidified N_2.

The selectivity of CO_2 in the decomposition products (CO and CO_2) was plotted in Figure 2.12. as a function of input power. The effect of water vapor on the removal of benzene with ferroelectric packed bed reactor, a portion of oxygen species in catalyst ($BaTiO_3$) was deactivated by adsorption of H_2O on their surfaces which resulting in suppress the formation of N_2O and CO thereby increase the selectivity of CO_2
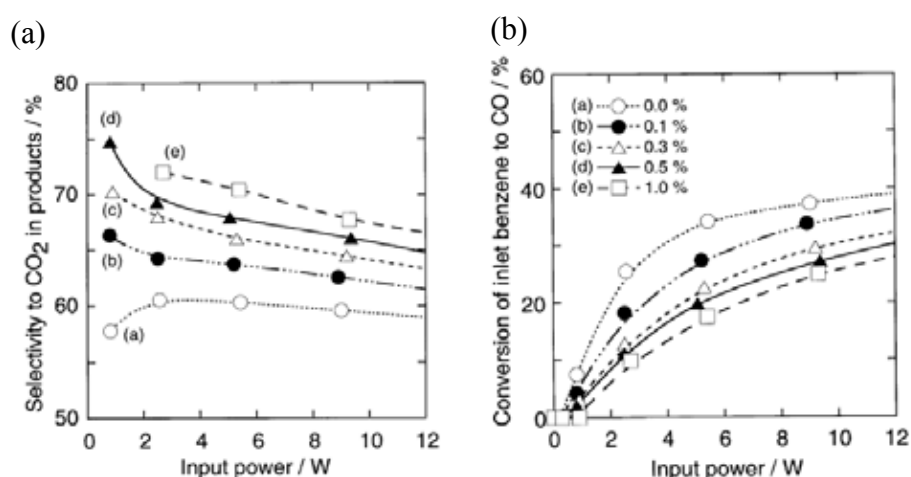
Figure 2.12 (a) Relationship between CO_2 selectivity with input power at various H_2O (%) ; (a) 0, (b) 0.1, (c) 0.3, (d) 0.5, and (e) 1.0. (b) Conversion of inlet to CO at various concentrations of H_2O (%) ; (a) 0, (b) 0.1, (c) 0.3, (d) 0.5, and (e) 1.0.

Li, *et al*., (2002) have investigated the improvement in the decomposition of Volatile Organic Compounds (VOCs) which combining discharge plasma with photocatalyst (TiO₂). Corona discharge was used for the generation of process plasma. Toluene ($C_6H_5CH_3$) was chosen due to typical VOCs existed not only in paint industry but also in house.
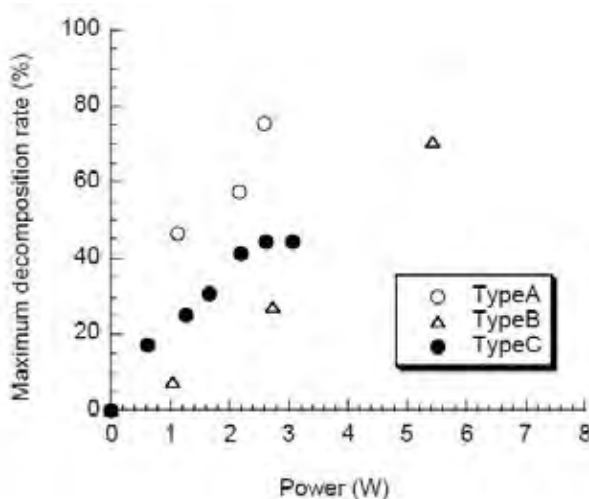
Figure 2.13 Maximum toluene decomposition rate as a function of power.

The decomposition of toluene was enhanced in the type A reactor with low power consumption. It seemed that the gas-phase toluene and the toluene adsorbed on the TiO_2 were decomposed simultaneously. In addition, TiO_2 activated by plasma may induce catalytic reactions. It was reported that ozone played the important role for the activation of TiO_2. Moreover, after turning off the power the outlet concentrations in both the type A and type B reactors remain low compared to the type C reactor. Due to the desorption process during the discharge, the surface condition of the catalyst may be recovered. From this result, it was considered that the plasma reactor with catalyst can be operated intermittently for improving the energy efficiency.

Lee, *et al*., (2004) used the plasma to decompose 100 ppm of benzene. In the experiment, they have performed with different catalyst loading amounts at hybrid system. Contrary to their expectation, they showed maximum conversion, that is, over 10% for plasma only system and at steady state which are almost similar to each other

as shown in Figure 2.14. (a). From this result, they thought that the photocatalyst induce complete oxidation of benzene. This reason would be supported by CO_2 selectivity. Figure 2.14. (b) shows that CO_2 selectivity increase about 70% compared with plasma only process. Accordingly, from those results, it might be concluded that photocatalysts on plasma process enhance benzene decomposition and at the same time guide to be completely oxidize to CO_2.

(a)   (b)
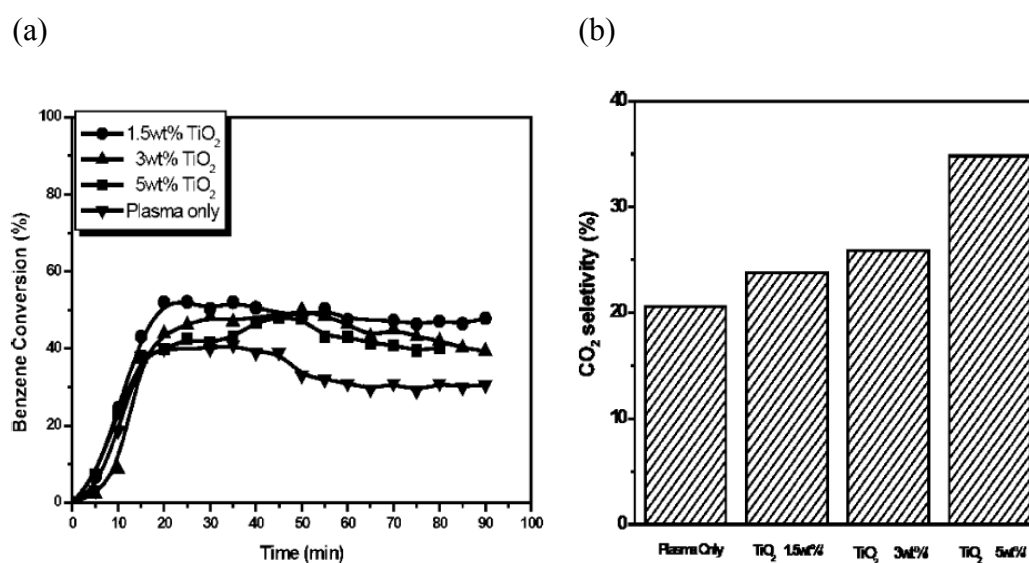
Figure 2.14 (a) Benzene decomposition activities in plasma photo-catalyst hybrid system with different loading amount. (b) CO_2 selectivity comparison for TiO_2 content effects in plasma–photocatalyst hybrid system.

Recently, as a practical approach to increase the residence time without increasing the size of the reactor, a macro-porous γ-Al_2O_3 which adsorbs VOCs selectively, has been suggested and reported that the emission of CO and N_2O from the process could be decreased with the γ-Al_2O_3 and the energy efficient removal process could be obtained Therefore, γ-Al2O3, which has been mainly used as a support of catalyst because it provides a good mechanical strength and high absorption ability, was used instead of glass bead.

Kim, *et al.*, (2005) have studied the Decomposition of gas-phase benzene using plasma-driven catalyst (PDC) reactor packed with Ag/TiO_2 catalyst due to the property of Ag that is also known to have capability of oxygen adsorption. the Ag loaded on TiO_2 catalysts by impregnation method is a metallic state rather than a metal oxide. These Ag catalysts of metallic state facilitate charge separation by trapping electrons and may lead to enhance the catalytic activity. Figure 2.15 shows a typical run of benzene decomposition using the PDC reactor with 1.0 wt.% Ag-loaded TiO_2 catalyst. Adsorption equilibrium over the Ag/TiO_2 catalyst bed reached within 40 min. As the plasma turned on, the concentration of benzene was decreased and those of CO and CO_2 were increased. The concentrations of benzene, CO and CO_2 showed some overshoots just after the SIE (specific input energy) conditions were changed, and then fell down to a steady value. The sum of CO and CO_2 accounts for most of the decomposed benzene.
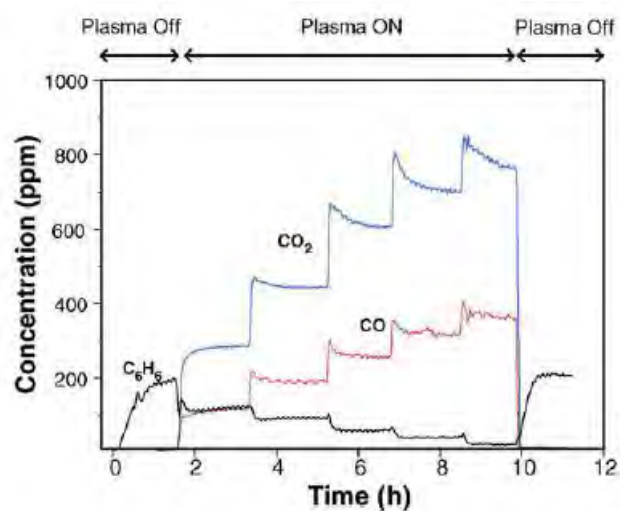
Figure 2.15 Typical runs of benzene decomposition using the PDC reactor. SIEs are 49.6, 100, 160, 197, 284 J/l respectively.

When the plasma was turned off, the concentration of benzene rapidly returned to its initial value and the formation of CO and CO_2 was stopped. These rapid responses to the plasma on/off confirm that the plasma induced catalytic activity is temporary one rather than lasting over a certain period after the plasma off. These data also suggested that the thermal catalysis was not important in the benzene decomposition because all the reactions stopped just after the plasma off.

Guo, *et al.*, (2010) have studied the effect of manganese oxide catalyst on the dielectric barrier discharge decomposition of toluene, as shown in Figure 2.16. (a) they found that toluene removal efficiency increases significantly when MnO_X catalyst is introduced into the discharge area. For example, with the catalyst in situ, the toluene removal efficiency (η) was 64.8% at a specific energy density (SED) of $50Wh/m^3$, which was two times more than that of 31.8% without catalyst. It also illustrates that the toluene removal efficiency increased with the increasing of SED whether catalyst exists or not. When SED was regulated from $39Wh/m^3$ to $89Wh/m^3$, η varied from 48.7% to 99.8% with MnO_X catalyst while η of 25.6–95.8% existed without catalyst. From Figure 2.16. (b) the selectivity of CO_2 is greatly enhanced by introducing a catalyst into the plasma reaction. Under the same SED of $89Wh/m^3$, the selectivity of CO_2 for DBD reactor was only 48.8% with no catalyst but it increased to 82.6% with the MnO_X catalyst. The selectivity was enhanced with active components due to the toluene oxidation near and/or on the catalyst surface. Maybe this is due to that oxygen active species are formed through the decomposition of O_3 on the surface of catalyst, and oxygen active species would further oxide CO and toluene (or intermediate reaction products) into CO_2. Therefore a higher CO_2 selectivity was achieved.

(a) (b)
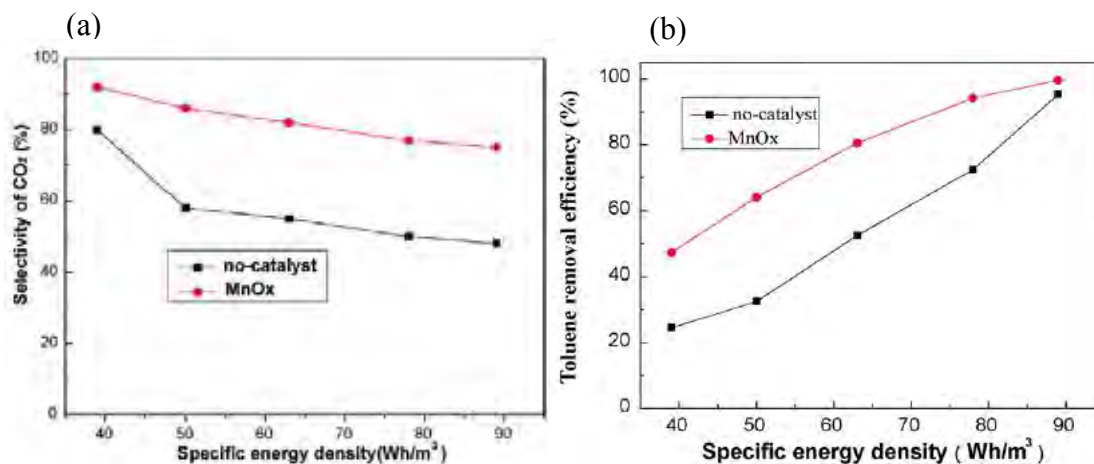
Figure 2.16 (a) Effect of specific energy density on the toluene removal efficiency with and without catalyst. (b) Influence of specific energy density on the selectivity of CO_2

In order to identify the specific type of manganese oxide (MnO_x) catalyst, TPR was used. As shown in Figure 2.17. These two peaks could be attributed to the two-step reduction of MnO_X. The first step corresponds to the reduction of MnO_2 to Mn_3O_4 and the second step is due to the further reduction of Mn_3O_4 to MnO. The reduction of $Mn_3O_4 + H_2 \rightarrow 3MnO + H_2O$ consumes more hydrogen than that of $3MnO_2 + H_2 \rightarrow 2Mn_3O_4 + H_2O$.
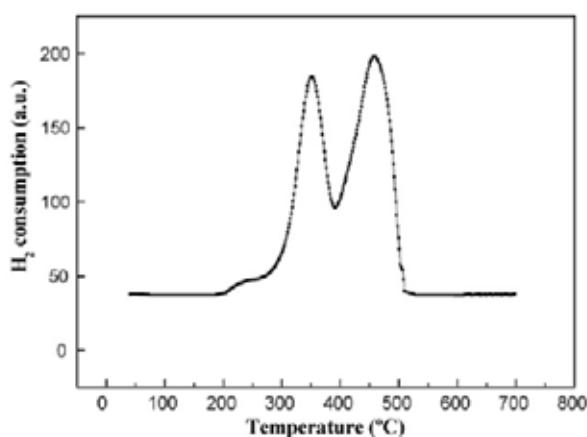
Figure 2.17 TPR curves for the MnO_X catalysts.

CHAPTER III
EXPERIMENTAL

3.1 Materials and Equipment

Equipment ;

1. Quartz tube reactor

2. Mass flow controller

3. Gas Chromatography machine

4. Syringe pump

5. Heater

6. Electrode

7. Thermocouple

Chemicals ;

1. Benzene (AR Grade)

2. Toluene (AR Grade)

3. Xylene (AR Grade)

4. He gas (UHP Grade)

5. Zero air (UHP Grade)

6. H_2 gas (UHP Grade)

7. Deionized water

3.2 Experimental Setup

The experimental system was divided into 5 sections: reactant-carried gas section feed, catalysts preparation, plasma reactor section, power supply section, and analytical section. Figure 3.1 shows the schematic of the experimental setup for benzene, toluene and xylene (mixed VOCs) oxidation reaction using corona discharge reactor.
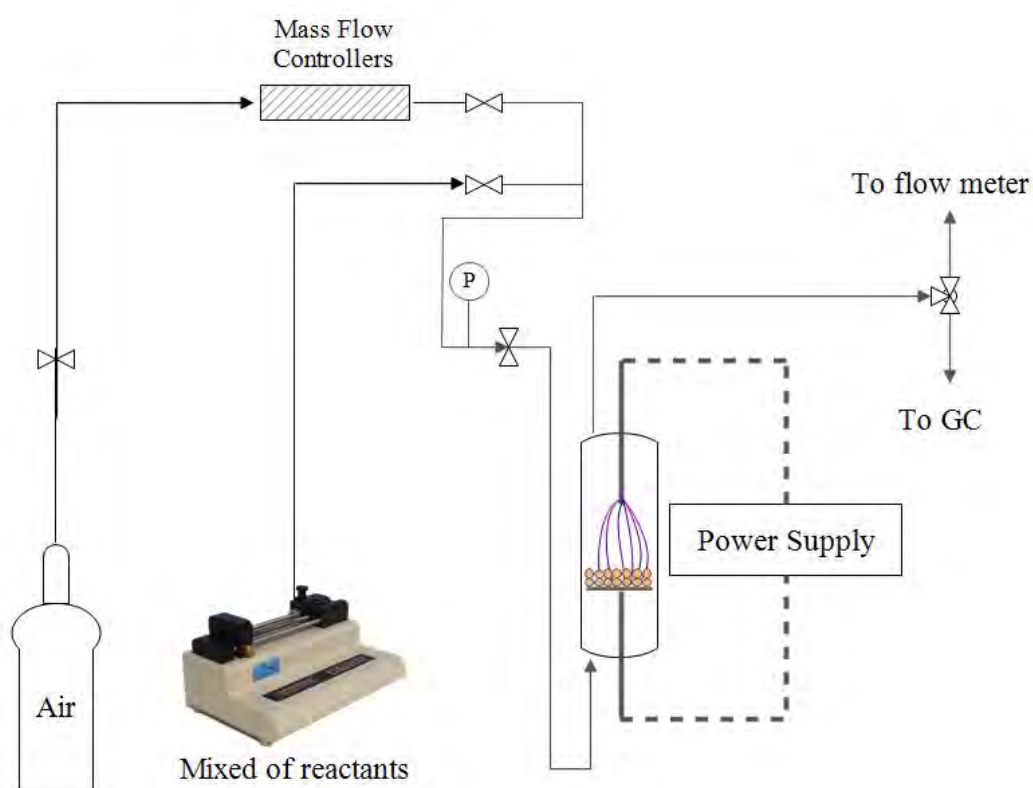
Figure 3.1 Experimental set up by using corona discharge reactors.

3.2.1 Reactant and Carried Gas Feed Section

The mixture of reactants which were benzene, toluene, and xylene were prepared at 1:1:1 by mass. The reactant concentration was achieved by vaporizing benzene, toluene and xylene (mixed VOCs) at a controlled temperature of 403 K. The flow rate of liquid mixed VOCs was controlled by a syringe pump supplied. In order

to prevent the any product condensation, the temperature of stainless tube in plasma reactors section to the GC detector was maintained at 403 K by using a heating cable.

The air flow rate were controlled by mass flow controller and transducer which were supplied by AALBORG. The check valve was also placed downstream of each mass flow controller to prevent any backflow.

3.2.2 Catalyst preparation section

From interesting metallic catalyst doped on support materials, there are already have the research grade for disperal Al_2O_3 and TiO_2 then for preparation section will be focused on dope metal trace on the support material instead.

3.2.2.1 Preparation of Ag/TiO₂

In order to prepare the TiO_2 coated on quartz wool, a sheet of quartz wool (1.5 cm × 1.5 cm) was prepared by impregnation method using a solution of 2 % Titanium (IV) oxide (TiO_2) in deionized water then held for 10 minutes at the room temperature. Afterwards, the coated quartz wool was dried at 378 K for 15 minutes, followed by calcination at 573 K for 3 hours .

After TiO_2 coated on quartz wool, the preparing of 0.5% - 5 % Ag/TiO₂ were prepared by using impregnation method which silver nitrate ($AgNO_3$) were used as a precursor. The coating procedure was the same as method described above except for the calcination temperature in this step is at 773 K for 10 hours.

3.2.2.2 Preparation of Ag/Al₂O₃

In order to prepare the Al_2O_3 coated on quartz wool, a sheet of quartz wool (1.5 cm × 1.5 cm) was first prepared by impregnation method using a solution of 2 % disperal alumina (Al_2O_3) in deionized water then held for 10 minutes in the room temperature. Afterwards, the coated quartz wool was dried at 378 K for 15 minutes, followed by calcination at 873 K for 3 hours.

After Al_2O_3 coated on quartz wool, the preparing of 0.5% - 5 % Ag/Al_2O_3 were prepared by using impregnation method which silver nitrate ($AgNO_3$) were used as a precursor. The coating procedure was the same as method described above except for the calcination temperature in this step is at 773 K for 10 hours.

3.2.2.3 Preparation of Mn/TiO_2

The coating of TiO_2 on coated quartz wool was the same as the preparation of Ag/TiO_2 method described above. The preparing of 0.5% - 5 % Mn/TiO_2 were prepared by using impregnation method which manganese chloride ($MnCl_2$) were used as a precursor. The coating procedure was the same as method described above.

3.2.2.4 Preparation of Mn/Al_2O_3

The coating of Al_2O_3 on coated quartz wool was the same as the preparation of Ag/Al_2O_3 method described above. The preparing of 0.5% - 5 % Mn/Al_2O_3 were prepared by using impregnation method which manganese chloride ($MnCl_2$) were used as a precursor. The coating procedure was the same as method described above.

3.2.3 Reactor Section

For the plasma oxidation of mixed VOCs, the non-thermal plasma reactor that used in this experiment was corona discharges which catalyst was located between pin and plate electrodes with the gap distance 15 mm. The reactor schematic is shown in Figure 3.2.

The corona discharge reactor consist of a 20-centimeter-long quartz tube with an outer diameter of 9 mm and an inner diameter of 7 mm. Plasma was generated between pin and plate electrodes, which were located at the center of the quartz tube reactor.
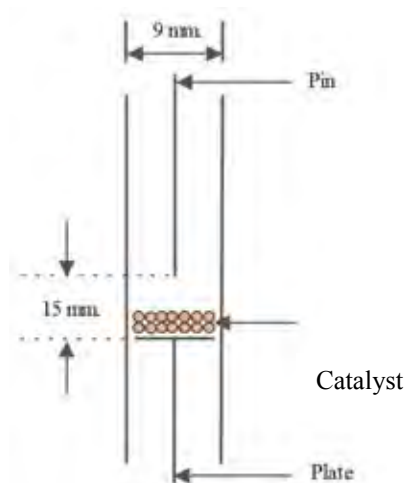
Figure 3.2 Configuration of corona discharge reactor.

3.2.4 Power Supply Section

The power supply unit consisted of three steps. For the first step, a domestic AC input of 220 V and 50 Hz was converted to a DC output of 70 V by a DC power supply converter. For the second step, a 500 W power amplifier with a function generator was used to convert the DC into AC current with a sinusoidal waveform and different frequencies. For the third step, the outlet voltage was stepped up by using a high voltage transformer. The output voltage and frequency were controlled by the function generator. The voltage and current at the low voltage side were measured instead of those at the high voltage side by using a power analyzer since the plasma generated is non-equilibrium in nature. The high side voltage and current were thereby calculated by multiplying and dividing by a factor of 15,000/220 ~ 68.2, respectively. Figure 3.3 shows the electric diagram of the power supply unit used in this study.
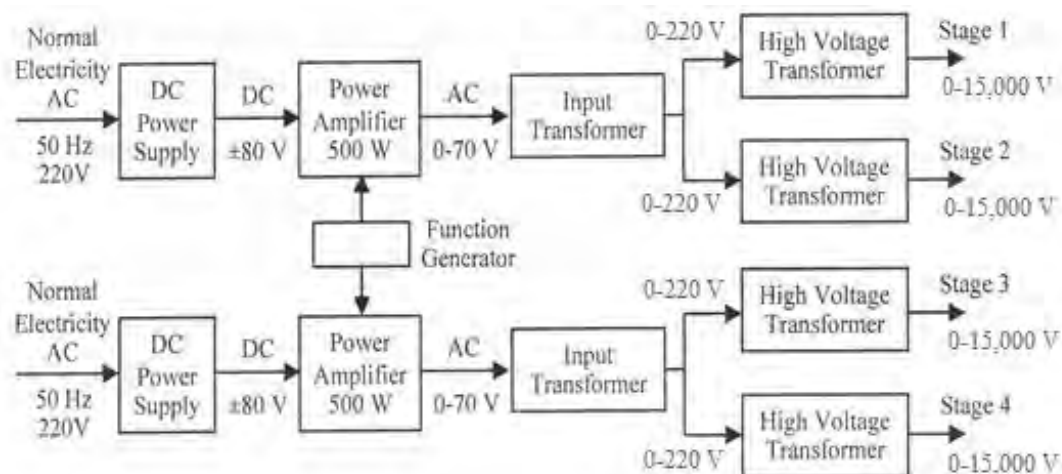
Figure 3.3 Schematic of the power supply unit.

3.2.5 Analytical Section

Composition of gas before and after the reaction in all experiments, the effluent gas samples were analyzed by an on-line gas chromatograph (HP, 5890) equipped with a Thermal Conductivity Detector (TCD) and a Flame Ionization Detector (FID). The quantitative analysis was carried out by correlating their peak area responses obtained from the GC chromatograms by calculating the percent volume of each component in outlet gas stream. The gas chromatography was equipped with a 10-port valve in order to separate the gas sample into two parts with independent sample loop. The first part was flow through a Carboxen 1000 column with the TCD. The second part was fed into a Rtx®-5 column connected with the FID. The GC conditions are summarized as follows;

Injector type :   Automatic sampling valve (programmable)

Injection temperature :   190ºC

Oven temperature :   Initial temperature 40ºC, ramp up at 10ºC/min
                          to 180ºC followed and then hold for 5 min

Detectors :	Thermal conductivity detector (TCD) and flame ionization detector (FID)
Detector temperature :	250ºC
GC columns :	Carboxen 1000 (15' x 1/8') and Rtx®-5 (30 m x 0.53 mm)
Carrier gas :	High purity helium (99.995%)
Carrier gas flow rates :	35 cm^3/min for Carboxen 1000 column and 105 cm^3/min for Rtx®-5 column

3.2.6 Catalyst Characterization

The characterization techniques consisted of Surface Area Analyzer Quantachrome Autosorb-1 (AS1-MP), Atomic absorption spectroscopy (AAS), Scanning electron microscopy (SEM), and X-ray photoelectron spectroscopy (XPS).

3.2.6.1 Surface Area Analyzer Quantachrome Autosorb-1(AS1-MP)

The surface area of the catalysts was determined to examine the effect of plasma on the catalyst. Surface area measurement was carried out by using Quantachrome Corporation Autosorb-1. The catalyst sample was out gassed to remove the humidity and volatile absorbents that adsorbed on surface under vacuum at 250 ºC at least 16 hours before performed the analysis with 26 points BET

3.2.6.2 Atomic absorption spectroscopy (AAS)

The actual metal loading on the TiO_2 and Al_2O_3 supports catalysts were analyzed by an atomic absorption spectrophotometer (AAS, Varian, Spectr AA-300).

3.2.6.3 Scanning Electron Microscopy (SEM)

Low vacuum SEM were used to study the surface morphology of the catalysts. Samples were dried in order to trap the humidity out, then the samples were place on a stub with carbon tape and coated by platinum. SEM created the picture by catching the signal from back scattering electrons with voltage of 2.0 kV and magnification of 2.50k.

3.2.6.4 X-ray Photoelectron Spectroscopy (XPS)

XPS technique was used to characterize metal species and oxidation states of metal on surface of catalysts. XPS was performed by using monochromatic Al source and pass energy at 20 and 160 for narrow and wide scan, respectively.

3.3 Experimental Procedure.

3.3.1 The Experimental System.

1) Set up the catalytic plasma reactor and all equipment to system as shown in Figure 5.1. Adjust the temperature controllers for heating line before input and output temperature of plasma reactor to 423 K and 473 K, respectively. Then, open zero grade air into plasma reactor.

2) Inject the prepare liquid mixed VOCs with concentration of 100 ppm by syringe pump with the constant flow rate of 0.7 ml/hr.

3) Adjust flow rate of zero air to 100 ml/min by digital mass flow controller. Measure feed flow rate before reaction outing from reactor by mass flow meter and analyze the composition of mixing gas by Gas chromatography.

4) Turn on power supply unit after it reach the steady state about 120 minutes and set applied voltage equal to 5 - 10 kV and frequency

400 - 500 Hz from function generator to plasma system, then observe the characteristics of plasma between electrodes.

5) The outlet gas compositions were continuously detect every 30 minutes until it reach steady state again.

6) Turn off power supply unit, close valves of zero air, turn off switch mass flow controller and gradually reduce temperature of temperature control.

7) Clean gas remaining in line pipe and reactor about 15 minutes.

8) Take off reactor, clean electrodes and surface inside the reactor.

3.4 Reaction Performance Evaluation

The plasma system performance was evaluated from VOCs conversions, CO_2 and CO selectivity and specific energy consumption. The conversion of reactant defined as follows ;

$$\text{Reactant conversion (\%)} = \frac{\text{Mole of reactant in - Mole of reactant out}}{\text{Mole of reactant in}} \times 100 \%$$

The selectivity of CO and CO_2 is calculated as follow ;

$$\text{Selectivity y of CO (\%)} = \frac{\text{Mole of CO in product}}{(6 \times \text{mole of Benzene removed}) + (7 \times \text{mole of Toluene removed}) + (8 \times \text{mole of Xylene removed})} \times 100 \%$$

$$\text{Selectivity y of } CO_2 \text{ (\%)} = \frac{\text{Mole of } CO_2 \text{ in product}}{(6 \times \text{mole of Benzene removed}) + (7 \times \text{mole of Toluene removed}) + (8 \times \text{mole of Xylene removed})} \times 100 \%$$

$$\text{Carbon balance of output product (\%)} = \frac{C_{Pi} \times P_i}{C_{Ri} \times R_i} \times 100 \ \%$$

Where P_i = Mass of product in the outlet gas stream.

R_i = Mass of each reactant in the feed stream.

C_{Pi} = The number of carbon atoms in a product molecule.

C_{Ri} = The number of carbon atoms in a reactant molecule.

The specific energy consumption is calculated in a unit of W.s per molecule of converted toluene using the following equation ;

$$\text{Specific Energy Consumption} = \frac{P \times 60}{N \times M_C}$$

Where P = Power measured at the low voltage side of the power supply unit (W).

N = Avogadro's number (6.02×10^{23} molecule g mole^{-1}).

M_C = Rate of converted carbon in the rate of produced CO_2 molecules (g mole min^{-1}).

CHAPTER IV
RESULTS AND DISCUSSION

The difference in operating parameters including applied voltage, input frequency, and type of catalysts could affect the performance of VOCs removal process and the production of desired product.

Figure 4.1 displays the chromatogram of condensed products analysis by GC-MS from oxidation reaction of mixed VOCs by corona discharge. From the previous study of Mr. Nitikorn Dithawat, 2018 under supervision of Prof. Sumaeth Chavadej, the condensed products were collected at an applied voltage of 4 kV, an input frequency of 600 Hz. The result indicated that there are two main collision steps consisting of electron collision and oxygen radical attraction.
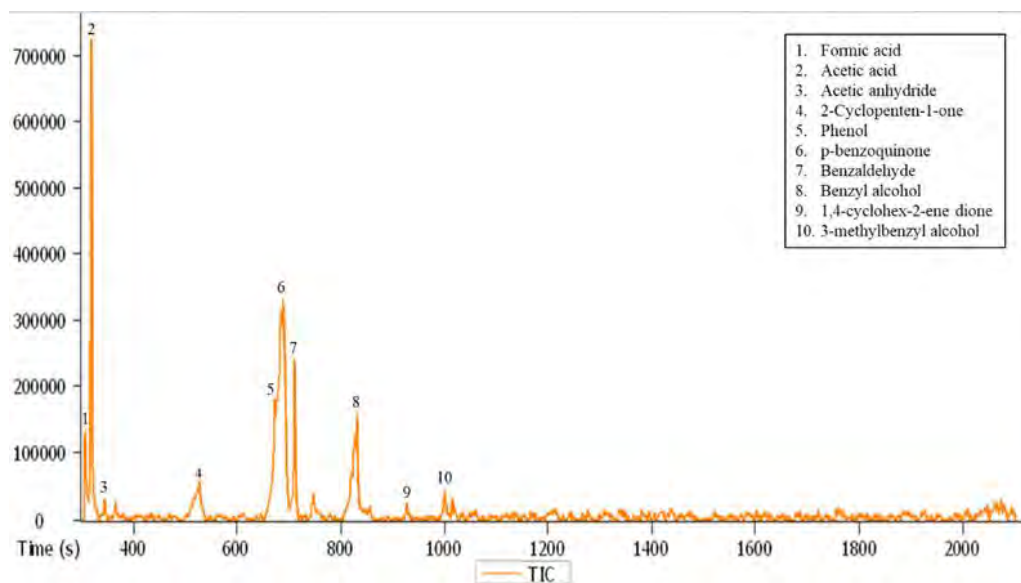
Figure 4.1 Chromatogram of GC–MS analysis for mixed VOCs degradation products by corona discharge at an applied voltage of 4 kV, an input frequency of 600 Hz, an initial concentration of 100 ppm and reactant feed flow rate of 100.0 ml/min.

Figure 4.2, the condensed products consisted of cyclic and noncyclic oxygenated molecules. The detected condensed products from GC-MS were in following order: formic acid, acetic acid, acetic anhydride, 2-cyclopente-1-one, phenol, p-benzoquinone, benzaldehyde, benzyl alcohol, 1,4-cyclohex-2-ene dione and 3-methylbenzyl alcohol. The main composition of condensed products was acetic acid. From the results, it could be confirmed that two earlier mention steps occurred because all condensed products contain at least one oxygen atom in molecule.
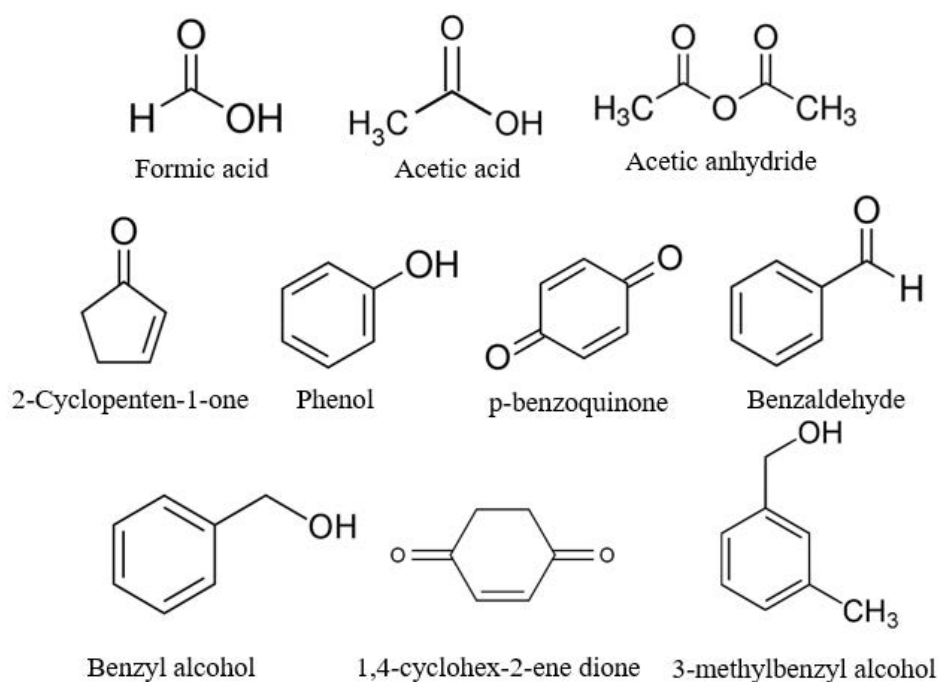
Figure 4.2 Summary of products of the studied mixed VOCs oxidation by corona discharge at an applied voltage of 4 kV, an input frequency of 600 Hz, an initial concentration of 100 ppm and reactant feed flow rate of 100.0 ml/min.

4.1 Sole plasma system

4.1.1 The effect of applied voltage

The applied voltage is one of important parameter for VOCs oxidation by plasma process. Fundamentally, the applied voltage plays important role on plasma behaviors and chemical reaction performance (Ondrats, *et al.*, 2017). In this study, plasma occurs at the lowest applied voltage of 4 kV. Due to the stability of plasma, the applied voltage can be varied from 5 - 10 kV. An initial VOCs concentration in air was 100 ppm, total feed flow rate of 100 ml/min, and gap distance between pin and plate electrodes of 15 mm.

4.1.1.1 Effect of applied voltage on reactant conversion

Figure 4.3 illustrates the effect of an applied voltage on VOCs conversion at different input frequency in the range of 400 - 500 Hz. When an applied voltage increased, the VOCs conversion increased at any studied input frequencies which corresponded to the Figure 4.4 that shows the effect of an applied voltage on measured current across electrodes, when an applied voltage increased from 5 to 10 kV, the current across electrodes will increase from 80 mA to 160 mA. The results can be explained by the fact that a higher applied voltage leading to higher produced electrons in a system that resulting in more VOCs conversion. The highest VOCs conversion of 98.3% was observed at an applied voltage of 10 kV.
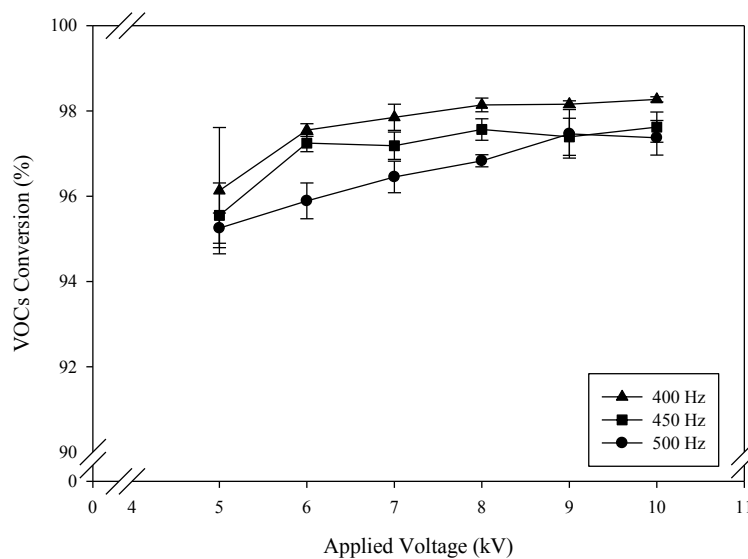
Figure 4.3 Effect of applied voltage on VOCs conversion at an initial VOCs concentration of 100 ppm, reactant feed flow rate of 100.0 ml/min, gap distance between pin and plate electrodes of 15 mm, and input frequency of 400 (▲), 450 (■), and 500 (●) Hz.
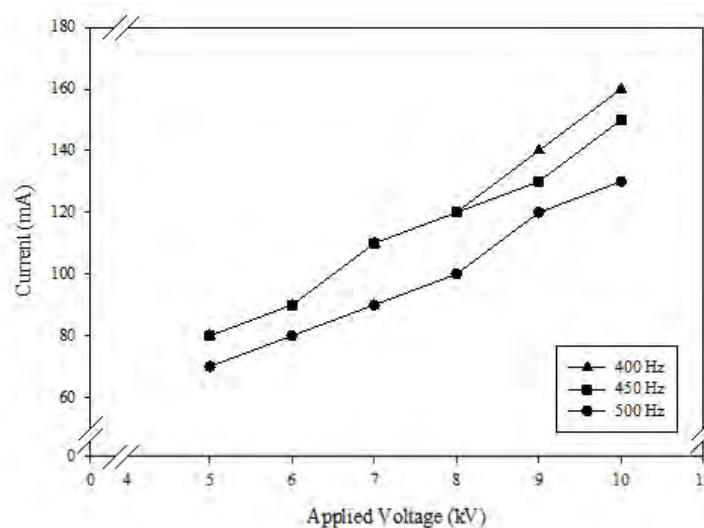
Figure 4.4 Effect of an Applied voltage on measured current across electrodes at an initial VOCs concentration 100 ppm, reactant feed flow rate of 100.0 ml/min, gap distance between pin and plate electrodes of 15 mm, and input frequency of 400 (▲), 450 (■), and 500 (●) Hz.

Figure 4.5 expresses the effect of an applied voltage on individual reactant conversion (dash line) and VOCs conversion (solid line) at an applied voltage of 10 kV and input frequency of 400 Hz. Results showed that at any studied applied voltage, the conversion were in following order: xylene, toluene, and benzene. Lee and colleagues found that toluene has a collision opportunity with generated electron to produce both $C_6H_4CH_3$ and C_6H_8 molecules as products and $C_6H_4CH_3$ molecules has a collision opportunity to produce only C_6H_6 molecules. Therefore, the xylene conversion would higher than toluene and benzene conversion respectively as well as at an applied voltage of 10 kV. At an applied voltage of 10 kV, benzene, toluene, xylene, and VOCs conversion found to be 96.7%, 98.6%, 99.6%, and 98.3% respectively.
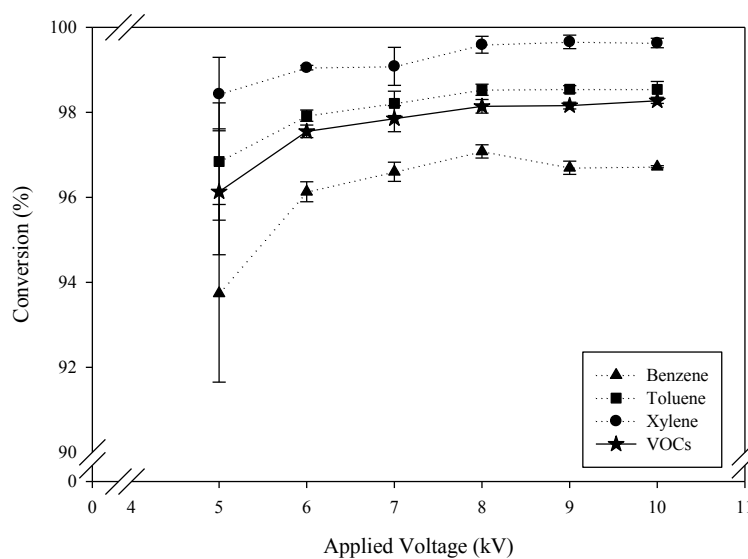
Figure 4.5 Effect of an applied voltage on individual reactant conversion (dash line) of benzene (▲), toluene (■), xylene (●), and VOCs conversion (solid line) (★) at an initial VOCs concentration of 100 ppm, reactant feed flow rate of 100.0 ml/min, and gap distance between pin and plate electrodes of 15 mm, and input frequency of 400 Hz.

4.1.1.2 Effect of an applied voltage on CO and CO_2 selectivities

Figure 4.6 shows the effect of an applied voltage on CO and CO_2 selectivities. When an applied voltage increased, the VOCs conversion and CO_2 selectivity increased whereas CO selectivity decreased. Besides, an applied voltage remains to promote a strong electric field strength across the electrodes. In particular, the electric field strength directly corresponds to both the electron density and input energy (current) in the plasma (Pornmai, *et al*., 2012). This phenomenon can be confirmed by the increasing in measured current across electrodes when an applied voltage was increased as shown in Figure 4.5. The increasing in current while an applied voltage was increase resulting the increasing of generated electrons provided the higher opportunity for VOCs molecules to react with generated electrons themselves and produced active species such as O^- leading to a higher VOCs conversion and CO_2 selectivity (Chavadej, *et al*., 2007). According to the increasing of current in system, CO which can be considered as by product of this oxidation reaction also further reacted with produced active species and further produced CO_2 resulting to the increasing of CO_2 selectivity. Therefore, at an applied voltage of 10 kV and input frequency of 400 Hz showed the good VOCs oxidation performance which provide high CO_2 selectivity which was 79.0% and low CO selectivity which was 11.3% respectively.
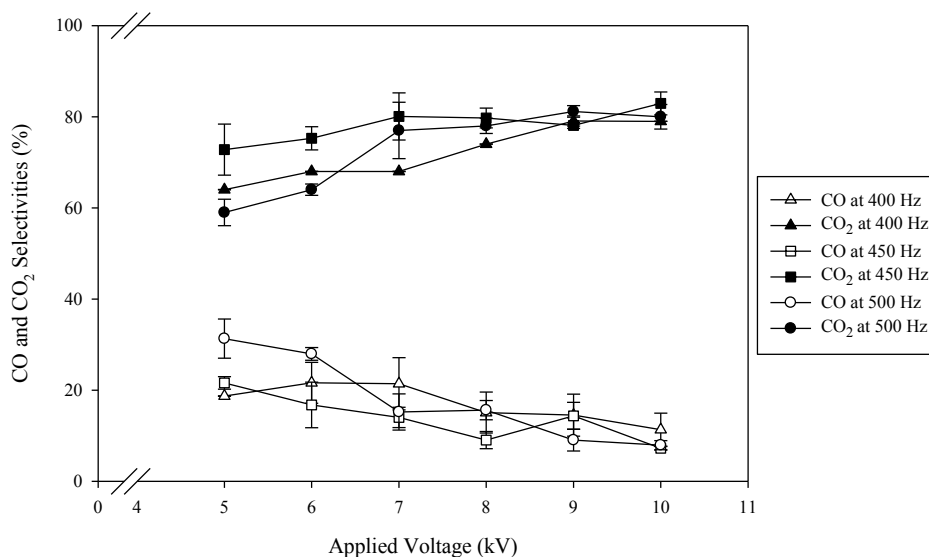
Figure 4.6 Effect of an applied voltage on CO selectivity (transparent symbols) and CO_2 selectivity (opaque symbols) at different input frequency of 400 (▲, Δ), 450 (■, □), and 500 (●, ○) Hz and an initial VOCs concentration of 100 ppm, reactant feed flow rate of 100.0 ml/min, gap distance between pin and plate electrodes of 15 mm.

4.1.2 The effect of input frequency

The input frequency has significantly impacts to the electric field strength in the plasma zone. According to the limitation of the operational, the lowest frequency that plasma occurred was 350 Hz and the highest input frequency was 550 Hz. Due to coke formation leading to non-stable plasma formation, in this study, the input frequency will be varied in the range of 400 to 500 Hz. Whereas other operating parameters including an initial VOCs concentration in air was 100 ppm, total feed flow rate of 100 ml/min, gap distance between pin and plate electrodes of 15 mm were fixed respectively.

4.1.2.1 Effect of input frequency on reactant conversion

Figure 4.7 illustrates the effect of input frequency on VOCs conversion at different applied voltage. An applied voltage was varied in the range of 4 – 10 kV. At any applied voltage, the VOCs conversion decreased with an increasing of input frequency. According to the basic concept of the frequency which affect to the characteristics of alternating current discharge by changing the plasma reaction performance and behaviors (Chavadej, *et al.*, 2006). For alternating current system, frequency represent the cycle loop over time to change polarity from positive to negative and from negative to positive between electrodes within a short time. The lower frequency, the lower reversal rate of electric fried leading to the higher current in plasma system which resulted to the increasing of collision opportunity between electrons and O_2 molecules. Therefore, there are more active species in the system which further react with VOCs molecules (Chang, *et al.*, 1991). At any applied voltage, the input frequency of 400 Hz provided the highest VOCs conversion which was 98.3% at an applied voltage of 10 kV that correspond to Figure 4.8 that illustrated the measured current across electrodes at an applied voltage of 10 kV was found to be decreased from 160 mA to 130 mA with increasing of the input frequency from 400 to 500 Hz.
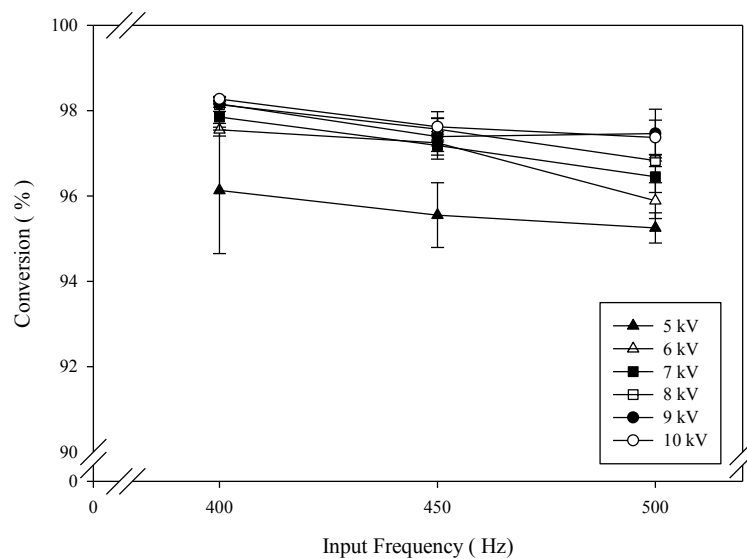
Figure 4.7 Effect of input frequency on VOCs conversion at different applied voltage of 5 (▲), 6 (Δ), 7 (■), 8 (□), 9 (●), and 10 (○) kV and an initial VOCs concentration of 100 ppm, reactant feed flow rate of 100.0 ml/min, gap distance between pin and plate electrodes of 15 mm.
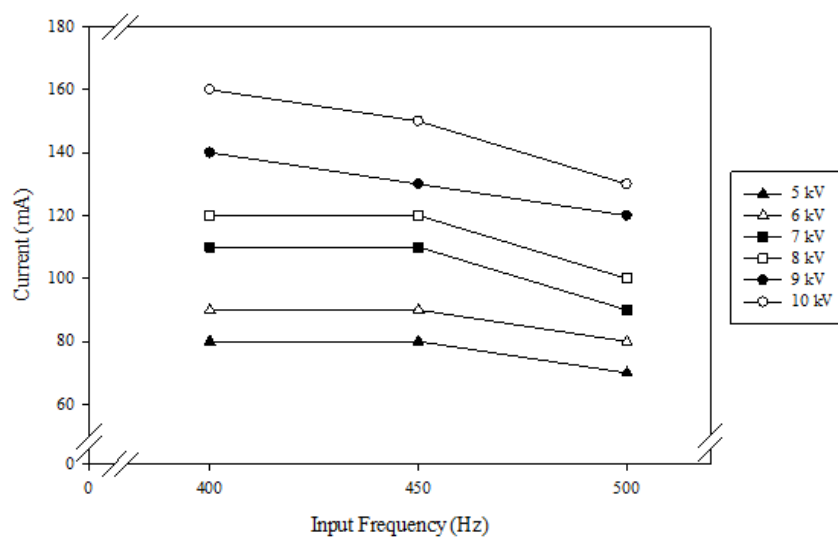
Figure 4.8 Effect of an input frequency on measured current across electrodes at different applied voltage of 5 (▲), 6 (Δ), 7 (■), 8 (□), 9 (●), and 10 (○) kV and an initial VOCs concentration of 100 ppm, reactant feed flow rate of 100.0 ml/min, gap distance between pin and plate electrodes of 15 mm.
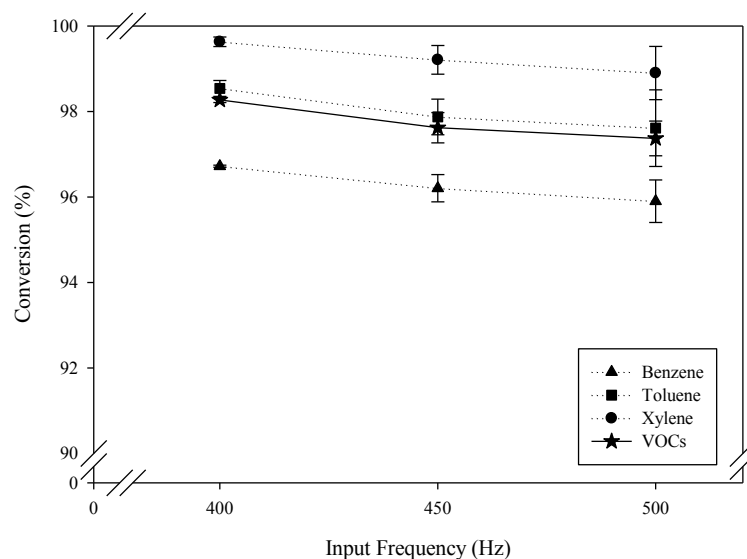
Figure 4.9 Effect of input frequency on individual reactant conversion (dash line) which composed of benzene (▲), toluene (■), xylene (●) and VOCs conversion (solid line) (★) at an initial VOCs concentration of 100 ppm, reactant feed flow rate of 100.0 ml/min, and gap distance between pin and plate electrodes of 15 mm, and an applied voltage of 10 kV.

Figure 4.9 illustrates effect of input frequency on individual reactant conversion (dash line) and VOCs conversion (solid line) at an applied voltage of 10 kV and input frequency of 400 − 500 Hz. Results showed that at any studied input frequency, the conversion were in following order: xylene, toluene and benzene. According to the proposed mechanism, there are three path ways of reaction in plasma zone consisting of electron collision, ion attraction and oxygen radical attraction. By the way, there were only main existing steps which were electron collision and oxygen radical attraction. In electron collision step, there was an opportunity of collision between xylene molecules and generated electron which produce both of $C_6H_4CH_3$ and C_6H_6. For toluene molecules, they probably collided with generated electrons and had an opportunity to produce C_6H_6 (Lee, *et al.*, 2002). At studied condition, benzene, toluene, xylene, and VOCs conversion at an input frequency of 400 Hz were found to be 96.7%, 98.5%, 99.6%, and 98.3% respectively.

4.1.2.2 Effect of input frequency on CO and CO_2 selectivities

Figure 4.10 expresses the effect of input frequency on CO and CO_2 selectivities. The increasing of input frequency resulting in decreasing of CO_2 selectivity but CO selectivity increased. As confirmed in Figure 4.11, the higher input frequency was the lower current lead to the less generated electrons and produced active species. Therefore, the reaction between produced active species and CO molecules did not occur frequently when compared to the system with higher current. Thus, at an input frequency of 400 Hz and applied voltage of 10 kV performed the appropriate performance considering from trace amount of CO selectivity.
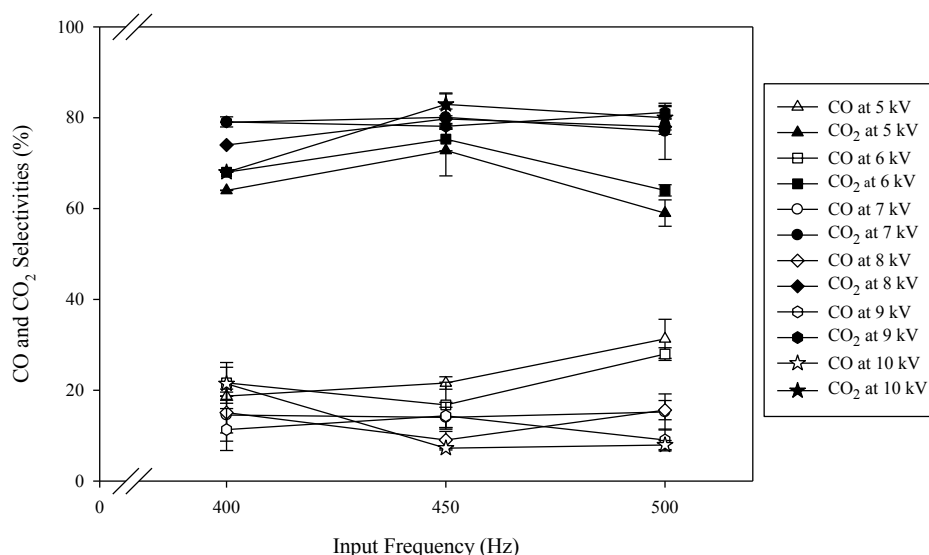
Figure 4.10 Effect of input frequency on CO_2 and CO selectivities. at an applied voltage of 5 (▲, △), 6 (■, □), 7 (●, ○), 8 (◆, ◇), 9 (◖, ◯), and 10 (★,☆) kV and an initial VOCs concentration of 100 ppm, reactant feed flow rate of 100.0 ml/min, gap distance between pin and plate electrodes of 15 mm.

Among all operating conditions, at an applied voltage of 10 kV and input frequency of 400 Hz provided the highest VOCs conversion of 98.3%, high CO2 selectivity of 79.1% and low CO selectivity which was 11.3% respectively. In this work, an operating condition in this study were selected in condition that an applied voltage of 5 kV, input frequency of 500 Hz which provided the VOCs

conversion of 95.3%, CO2 selectivity of 59.0% and CO selectivity of 31.3% due to investigate the effect of catalyst on VOCs conversion and product selectivity.

4.2 The effect of the presence of catalysts

Metal oxides are usually employed as a support for metal catalysts. It is well known that the adhesion and interaction between the metal particles and the support are important factors that influence the stability, activity and selectivity of a catalyst (Kizling, *et al*., 1996). The techniques of surface modification, for example plasma, can be useful in order to improve the adhesion or to modify interaction between metal and support. The operational conditions in this study were kept at an initial VOCs concentration of 100 ppm, reactant feed flow rate of 100.0 ml/min, gap distance between pin and plate electrodes of 15 mm, an applied voltage of 5 kV, an input frequency of 500 Hz.

4.2.1 Catalysts characterization

The catalysts with various loadings of Ag and Mn on TiO_2 and Al_2O_3 supports coated on quartz wool were prepared by impregnation method and calcined at temperature of 550°C. The characteristic of catalysts were determined by Brunauer-Emmett-Tellet (BET) surface area analyzer, Atomic Absorption Spectroscopy (AAS), X-ray photoelectron spectroscopy (XPS), and Scanning electron microscopy (SEM).

4.2.1.1 Brunauer-Emmett-Tellet (BET) Surface Area Analysis and Atomic Absorption Spectroscopy (AAS)

The N_2 adsorption-desorption isotherms were obtained by a Brunauer-Emmett-Tellet (BET) surface area analyzer to determine the specific surface areas of all catalysts. Each catalyst sample was firstly outgassed at 250 °C for 17 h to remove the humidity and volatile species adsorbed on the surface before analysis. The actual metal loadings on the synthesized catalysts were analyzed by an atomic absorption spectroscopy (AAS). The BET specific surface area values and the actual

amounts of loaded metal contents on the studied catalysts are listed in Table 4.1. The results show that the increasing of metal loading on the supports correspond to the decreasing of surface area of catalyst.

Table 4.1 BET surface areas and actual metal contents of all studied catalysts

Catalyst	BET Surface Area (m^2/g)	Actual metal content (wt %)
TiO_2	45.0	-
Al_2O_3	172.5	-
1% wt AgO_x/TiO_2	38.8	0.8
5 % wt AgO_x/TiO_2	16.8	4.2
1% wt AgO_x/Al_2O_3	154.3	0.9
4% wt AgO_x/Al_2O_3	147.4	3.3
1 % wt MnO_x/TiO_2	31.9	0.7
5 % wt MnO_x/TiO_2	21.5	4.4
1 % wt MnO_x/Al_2O_3	155.2	0.8
5 % wt MnO_x/Al_2O_3	152.5	4.9

4.2.1.2 Scanning electron microscopy (SEM)

Scanning electron microscopy (SEM) was applied to capture the surface morphology of Ag and Mn on TiO_2 and Al_2O_3 support on coated quartz wool catalysts (TiO_2-supported and Al_2O_3-supported). The studied catalysts were dried in an oven for 24 h and kept in a desiccator before analysis. All images of studied catalyst were shown in Figure 4.11 - 4.15. Figure 4.11 displays the appearance of surface morphology of TiO_2 and Al_2O_3. The surface of Al_2O_3-supported had a smoother surface compared to the TiO_2-supported indicated that alumina was well dispersed on the surface of quartz wool while TiO_2-supported gave a higher clustered layers. As a result, Al_2O_3-supported showed good distribution leading to the higher specific surface area than TiO_2-supported which corresponded to the previous result of specific surface area analysis.

Figure 4.12 shows the appearance of surface morphology of 1% Ag/TiO$_2$ compared with 5% Ag/TiO$_2$. The result shows that when the Ag loading increased, the opportunity of Ag agglomeration increased which attributed to the large particle size of Ag. Therefore, the high percentage of metal loading directly affected to reduce the specific surface area of catalysts. These results can be confirmed by the previous section, the higher Ag loading, the lower specific surface area. Figure 4.13 shows the appearance of surface morphology of 1% Ag/Al$_2$O$_3$ compared with 4%Ag/Al$_2$O$_3$. Interestingly, increasing Ag loading (1% - 4%) has less effect to the surface morphology in terms of agglomeration as compared to the Ag/TiO$_2$ catalyst.

Figure 4.14 shows the appearance of surface morphology of 1% Mn/TiO$_2$ compared with 5% Mn/TiO$_2$. Since TiO$_2$-supported provided the clustered layers, the molecule of small round microparticles Mn were aggregated with each other which directly reduced the specific surface area of catalyst. Figure 4.15 shows the appearance of surface morphology of 1% Mn/Al$_2$O$_3$ compared with 5% Mn/Al$_2$O$_3$. The results found that at 5% Mn/Al$_2$O$_3$ there was a number of small round microparticles Mn attached on the surface of support higher than 1% Mn/Al$_2$O$_3$.
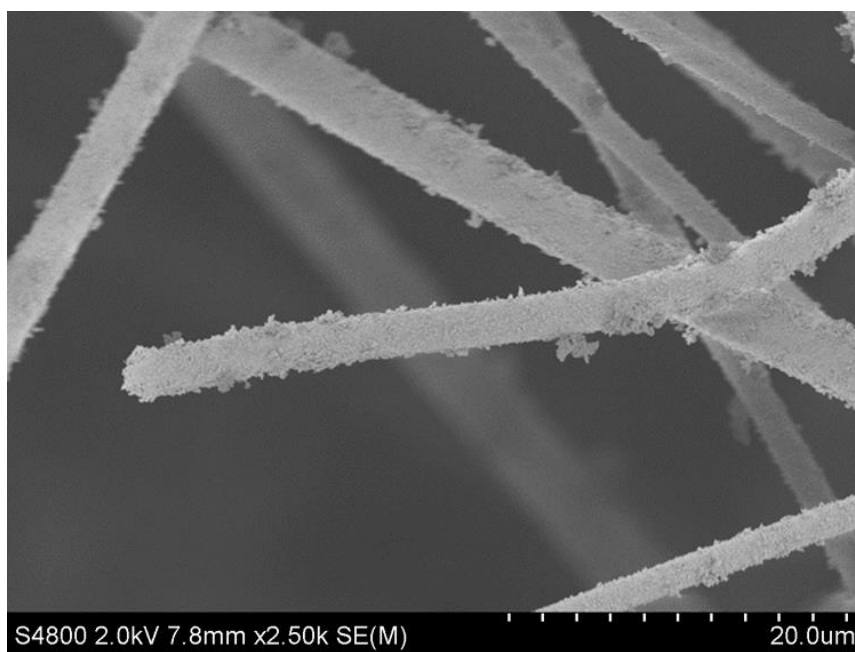
(a)
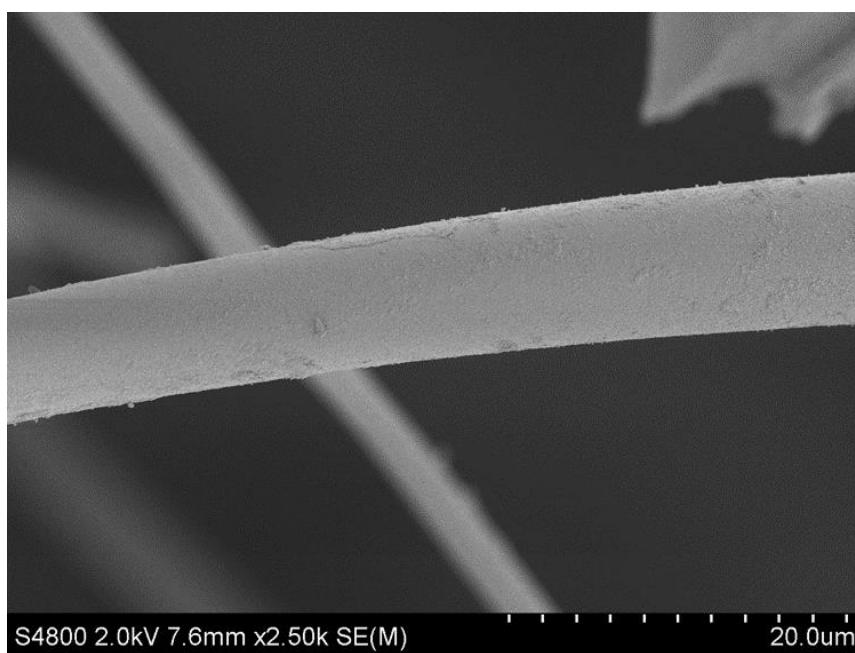
(b)

Figure 4.11 SEM image of (a) TiO$_2$ and (b) Al$_2$O$_3$ support on coated quartz wool
with the magnification of 2.5k
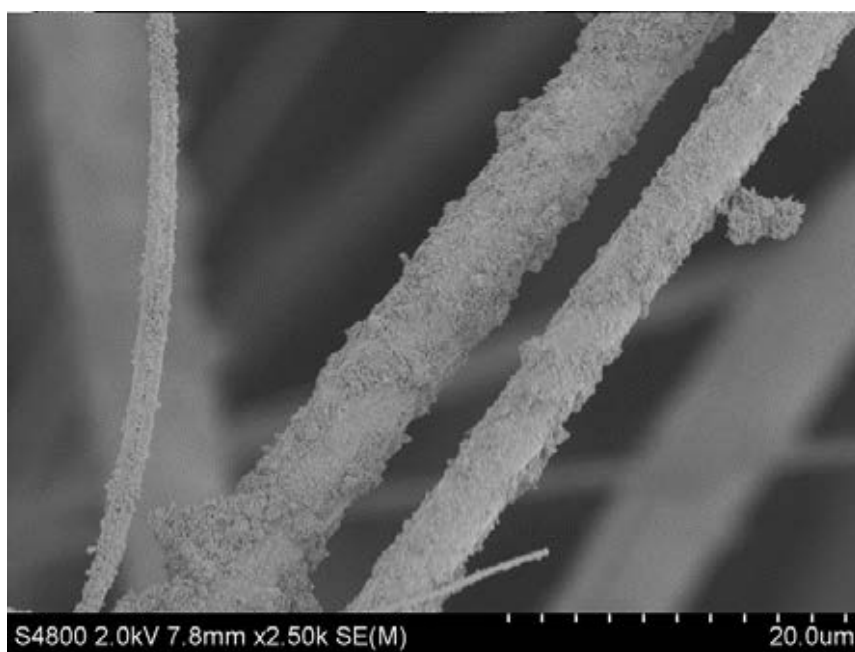
(a)
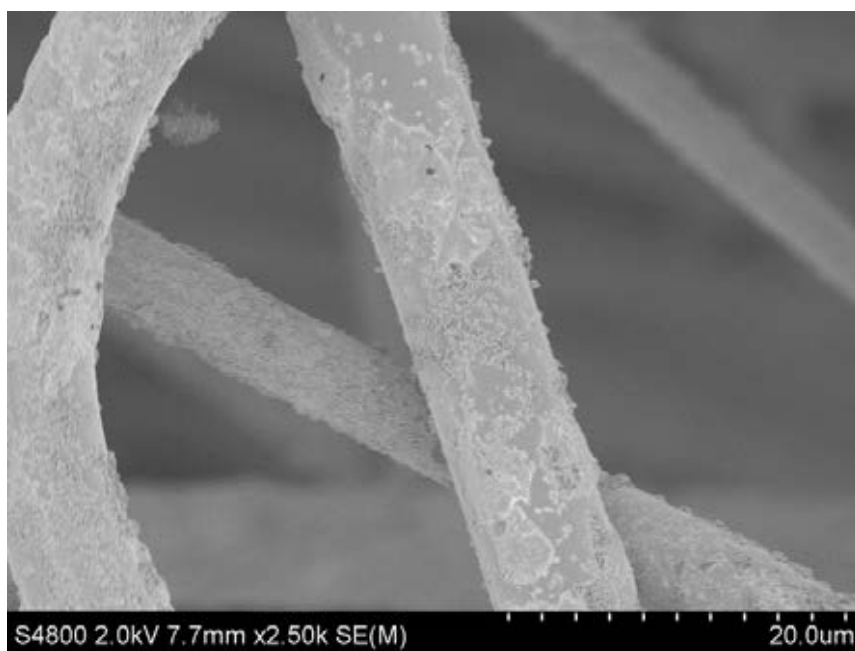
(b)

Figure 4.12 SEM image of various loading of Ag on TiO$_2$ support on coated quartz
wool with the magnification of 2.5k (a) 1% Ag/TiO$_2$ and (b) 5% Ag/TiO$_2$
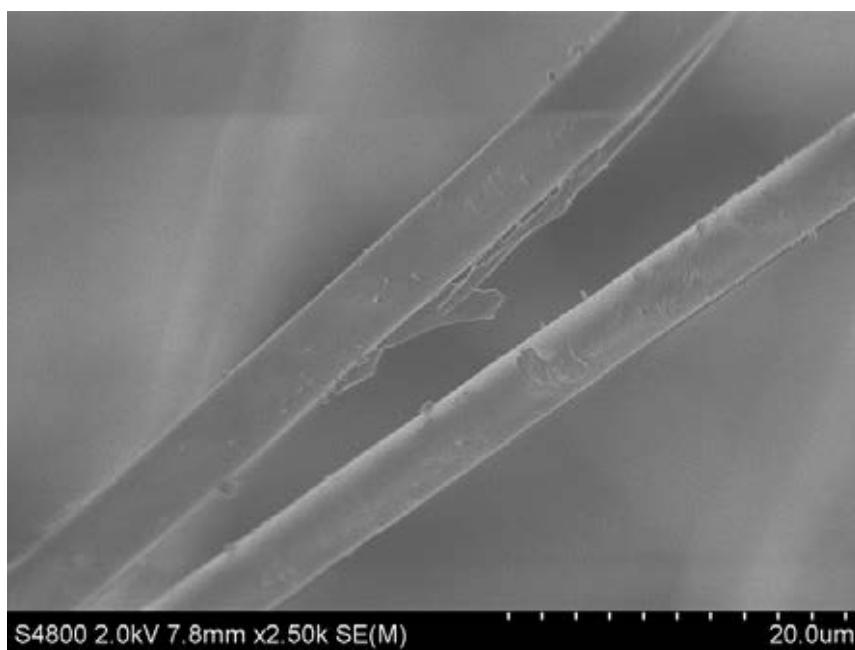
(a)
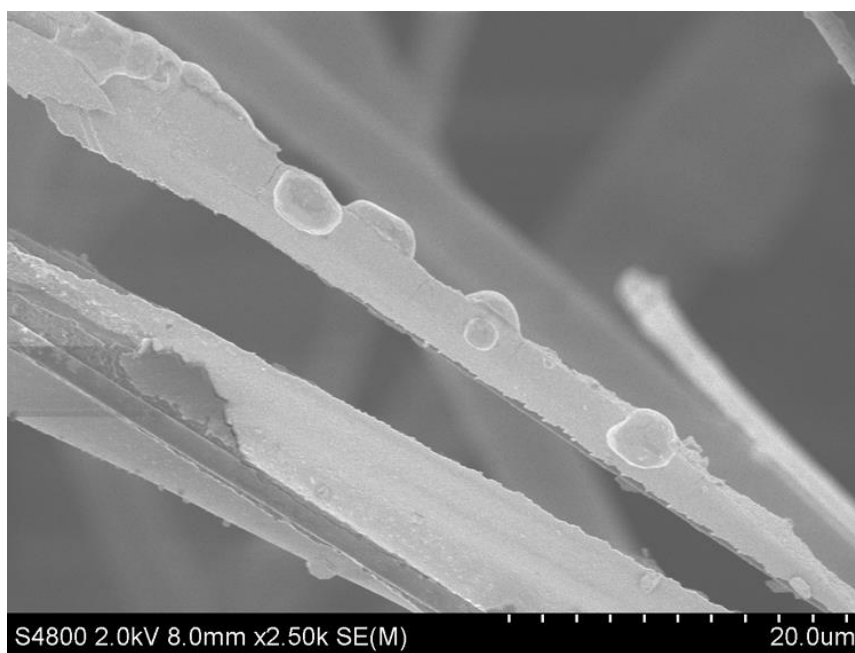
(b)

Figure 4.13 SEM image of various loading of Ag on Al_2O_3 support on coated quartz wool with the magnification of 2.5k (a) 1% Ag/Al_2O_3 and (b) 4% Ag/Al_2O_3
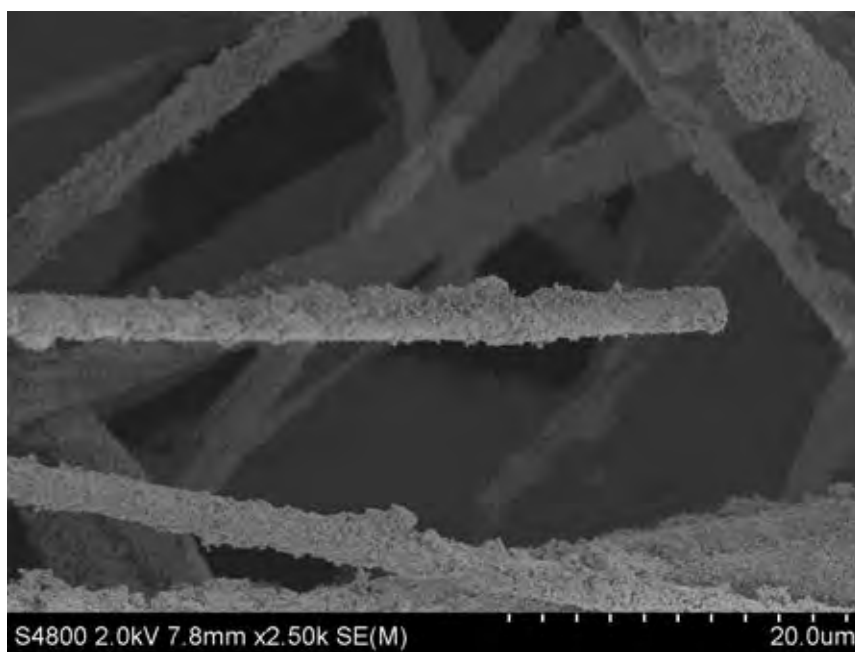
(a)
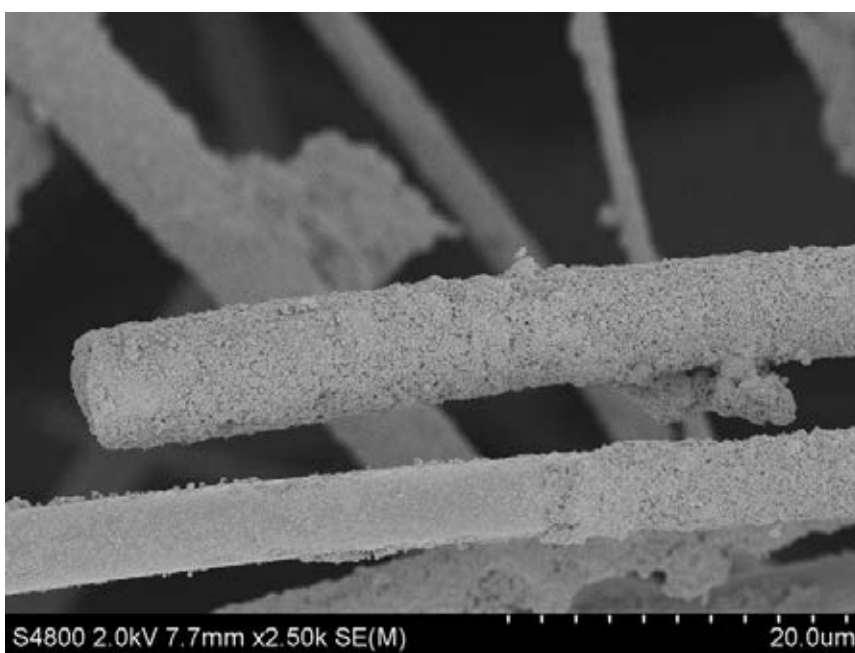
(b)

Figure 4.14 SEM image of various loading of Mn on TiO_2 support on coated quartz wool with the magnification of 2.5k (a) 1% Mn/TiO_2 and (b) 5% Mn/TiO_2
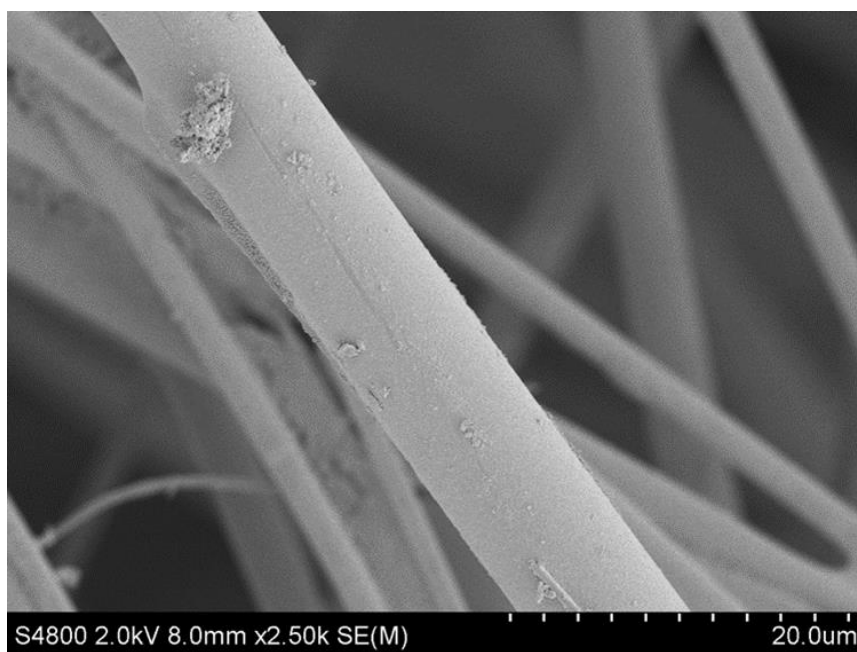
(a)
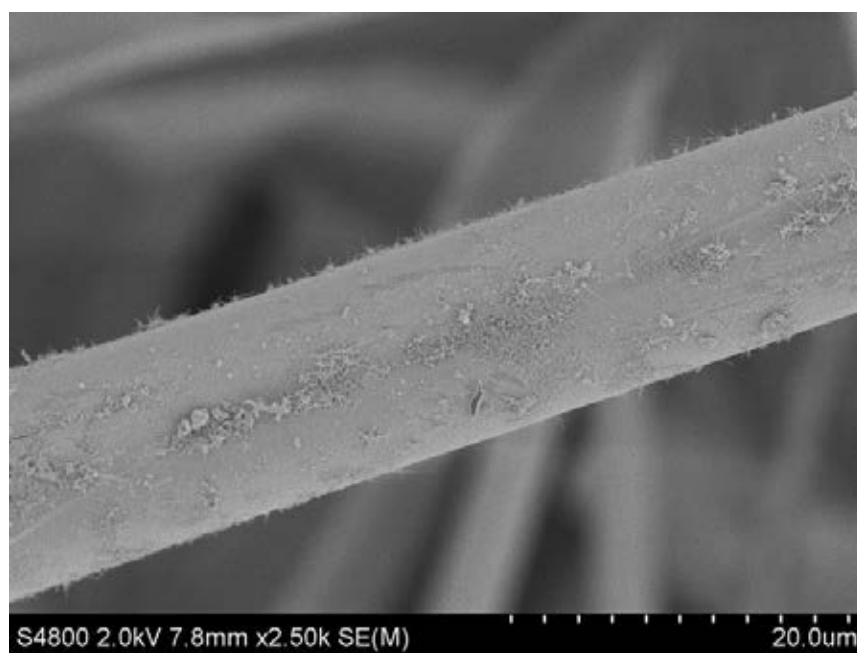
(b)

Figure 4.15 SEM image of various loading of Mn on Al_2O_3 support on coated quartz wool with the magnification of 2.5k (a) 1% Mn/Al_2O_3 and (b) 5% Mn/Al_2O_3

4.2.1.3 X-ray photoelectron spectroscopy (XPS)

In order to understand the surface atomic and oxidation states of Ag and Mn on TiO_2 and Al_2O_3 supports at various metal loadings. Figure 4.16 - 4.21 show XPS spectra of all studied catalysts. Figure 4.16 and 4.17 show spectrum of TiO_2 and Al_2O_3 support, the binding energies of Ti 2p of all studied catalysts were observed around 458 and 464 eV. Moreover, the binding energies of Al 2p of all studied catalysts were observed in the range of 73.4 - 74.7 eV which correlated to the Al 2p in gamma alumina phase (Strohmeier, *et al.*, 1995). Therefore the preparation of Al_2O_3 was synthesized in form of γ-Al_2O_3 because it got the binding energy in the range of with Al 2p in gamma alumina phase.

From XPS results, it indicated that there were many species of metal oxide consisting of silver metal (Ag), silver (I) oxide (Ag_2O), manganese (III) oxide (Mn_2O_3), manganese dioxide (MnO_2), and manganese (II,III) oxide (Mn_3O_4) detecting on catalyst surface of fresh and spent catalysts. For Ag metal, it showed characteristic peaks at binding energy of 368.18 and 374.27 eV which corresponded to Ag $3d_{5/2}$ and Ag $3d_{3/2}$. Additionally, the peaks at 368.40 and 374.00 eV were characteristic peak of Ag $3d_{5/2}$ and Ag $3d_{3/2}$ in Ag_2O. For MnO_2, the peaks at 643.40 and 653.90 eV indicated the Mn $2p_{3/2}$ and Mn $2p_{1/2}$ respectively. Mn_2O_3 represented the peaks at 641.70 and 653.70 eV which were Mn $2p_{3/2}$ and Mn $2p_{1/2}$ respectively. Mn3O4, found only in spent catalyst, showed characteristic peaks of Mn $2p_{3/2}$ and Mn $2p_{1/2}$ at 641.40 and 653.70 eV respectively (Chongterdtoonsakul, *et al.*, 2013).

Figure 4.18 illustrates the XPS spectra of Ag $3d_{5/2}$ and Ag $3d_{3/2}$ compared between fresh catalyst (A) and spent catalyst (B) of 5% Ag/TiO_2 catalysts. When compared between fresh and spent catalyst found that for the fresh catalyst, peaks of Ag_2O were occurred at the binding energy of 368.23 and 374.23 eV. Whereas the XPS spectra of spent catalyst was observed peaks of Ag 3d5/2 and Ag 3d3/2 at the binding energy of 368.48 and 374.48 eV which indicated that in Ag_2O forms and observed partial Ag metal forms that were occurred at the binding energy in both 368.99 and 374.85 eV. This could indicated that the oxide forms of Ag were reacted with other molecules in the system. Figure 4.19 displays the XPS spectra of Ag $3d_{5/2}$

and Ag $3d_{3/2}$ compared between fresh catalyst (A) and spent catalyst (B) of 4% Ag/Al$_2$O$_3$ catalysts, peaks of Ag$_2$O were occurred at the binding energy of 368.40 and 374.40 eV whereas observed peaks in spent catalyst observed in both Ag$_2$O and Ag metal in the binding energy of 368.43 and 374.48, 369.41 and 375.62 eV. As compared with previous support found that for both supports, they show the same results that some of Ag$_2$O changed to Ag.

Figure 4.20 shows the XPS spectra of Mn $2p_{3/2}$ and Mn $2p_{1/2}$ compare between fresh catalyst (A) and spent catalyst (B) of 5% Mn/TiO$_2$ catalysts. When compared between fresh and spent catalyst, the fresh catalyst consisted of peaks of Mn$_2$O$_3$ and MnO$_2$, MnO and MnO$_2$. Whereas the XPS spectra of spent catalyst was observed the additional characteristic peaks of Mn$_3$O$_4$. This could indicated that the oxygen in oxide forms of Mn were reacted with other molecules in the system represented by the changing of oxidation state of Mn in spent catalyst.

Figure 4.21 illustrates the XPS spectra of Mn $2p_{3/2}$ and Mn $2p_{1/2}$ of fresh catalyst (A) and spent catalyst (B) of 5% Mn/Al$_2$O$_3$ catalysts. When compared between fresh and spent catalyst, the fresh catalyst showed peaks of MnO$_2$. Whereas the XPS spectra of spent catalyst indicated both peaks of MnO$_2$ and Mn$_3$O$_4$ indicating that the oxygen in Mn oxide forms were reacted with other molecules in the system due to oxidation number of Mn of fresh catalyst change from 4^+ to 2^+ and 3^+.
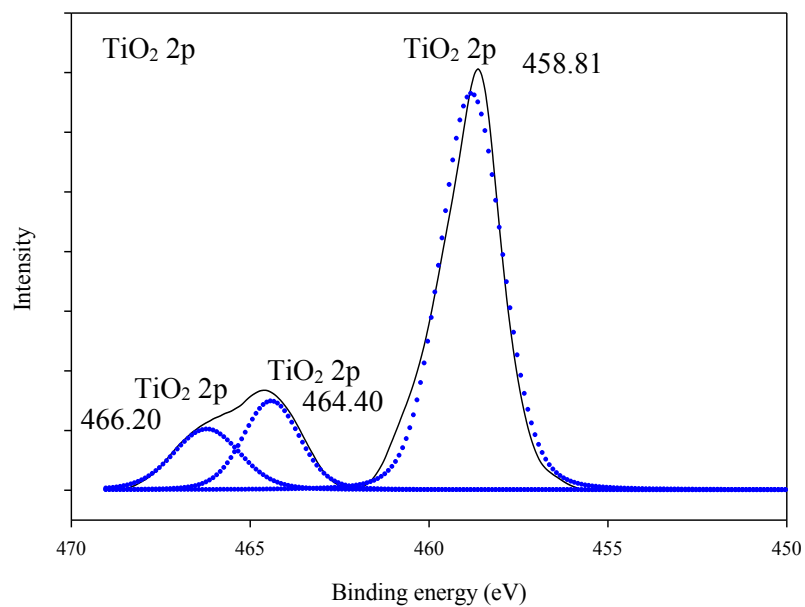
Figure 4.16 XPS spectra of Ti 2p on TiO_2 support.
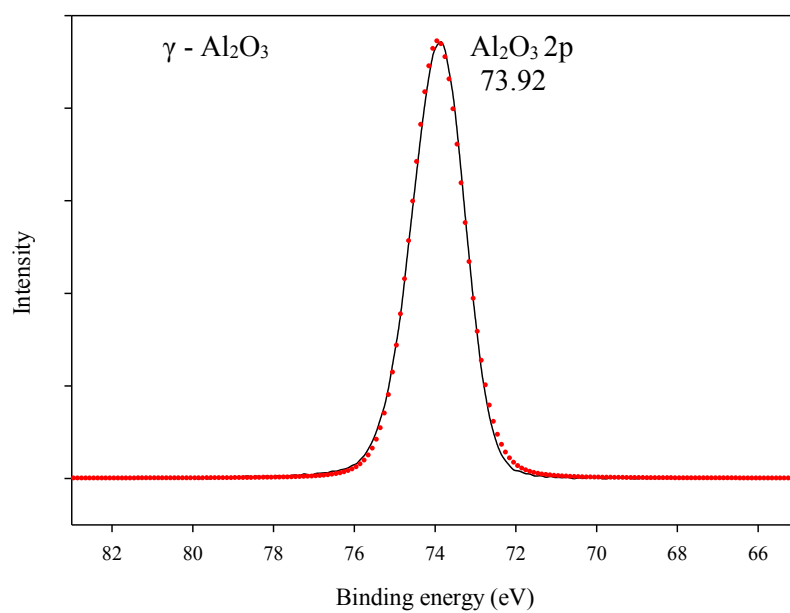
Figure 4.17 XPS spectra of Al 2p on Al_2O_3 support.
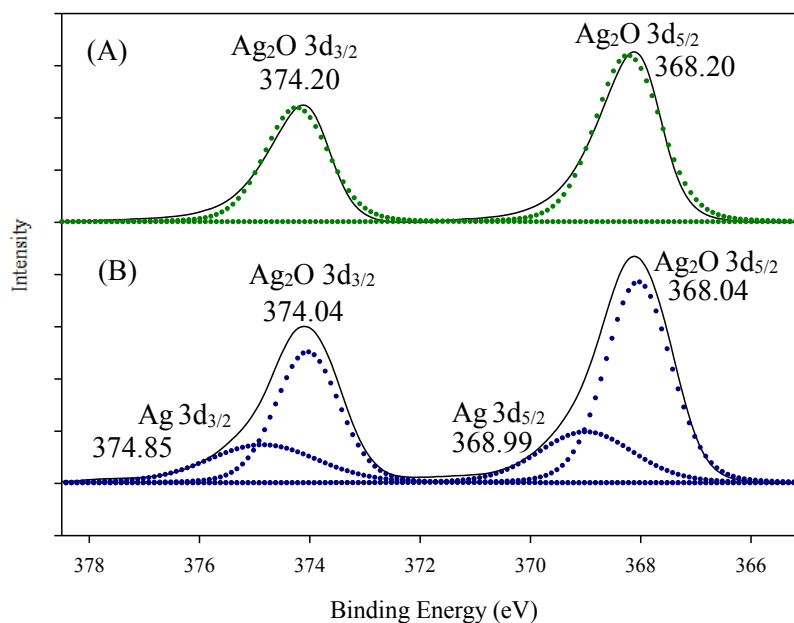
Figure 4.18 XPS spectra of Ag $3d_{5/2}$ and Ag $3d_{3/2}$ of fresh catalyst (A) and spent catalyst (B) of 5% Ag/TiO$_2$ catalysts.
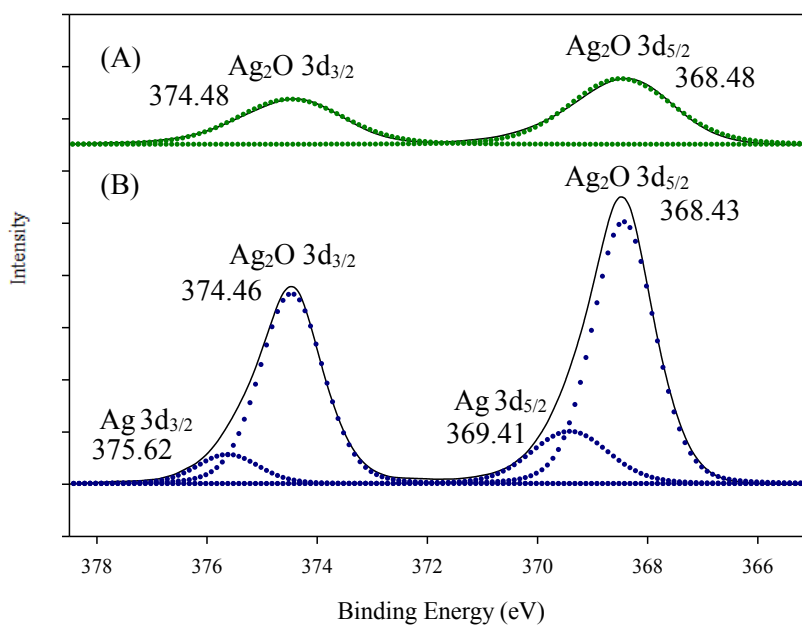
Figure 4.19 XPS spectra of Ag 3d5/2 and Ag 3d3/2 of fresh catalyst (A) and spent catalyst (B) of 4% Ag/Al$_2$O$_3$ catalysts.
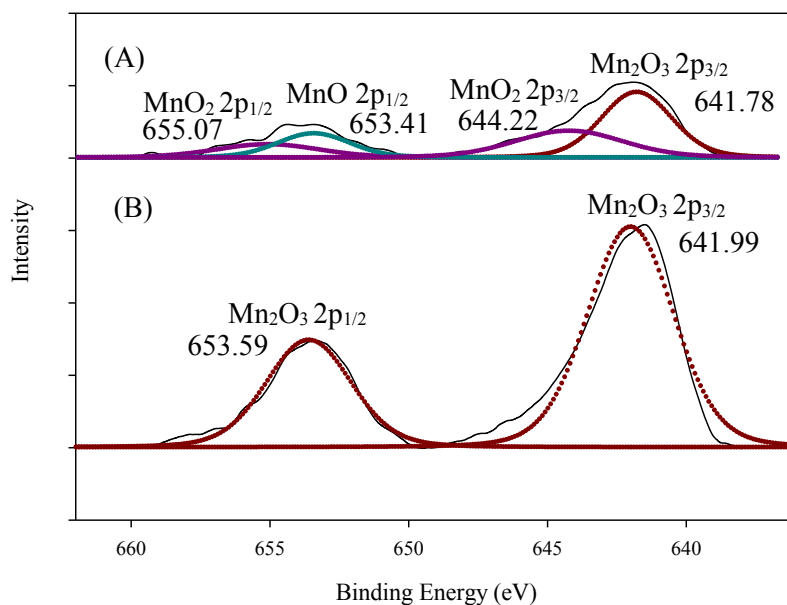
Figure 4.20 XPS spectra of Mn 2p$_{3/2}$ and Mn 2p$_{1/2}$ of fresh catalyst (A) and spent catalyst (B) of 5% Mn/TiO$_2$ catalysts.
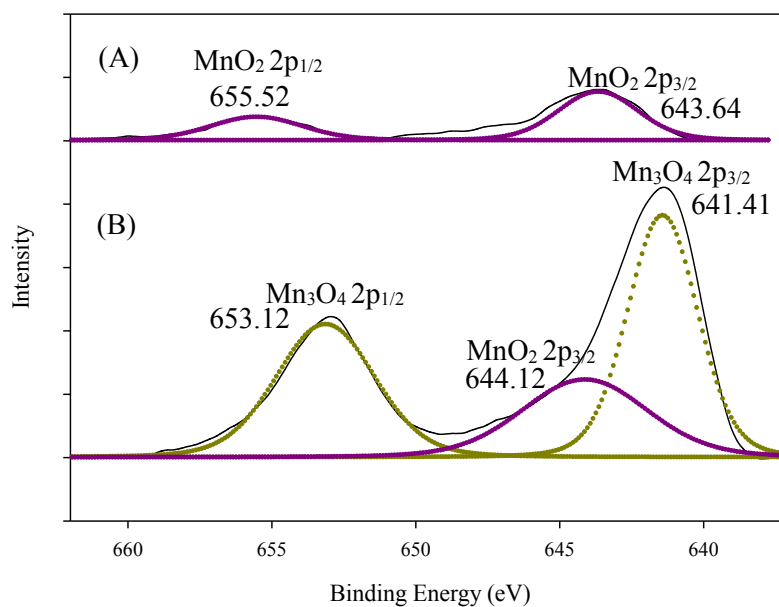
Figure 4.21 XPS spectra of Mn 2p$_{3/2}$ and Mn 2p$_{1/2}$ of fresh catalyst (A) and spent catalyst (B) of 5% Mn/Al$_2$O$_3$ catalysts.

4.2.2 <u>Effect of plasma catalytic activity testing on Ag/TiO_2 catalyst</u>

Ag is known as an oxidative catalyst for hydrocarbon. It was also reported that the Ag/TiO_2 catalyst has good performance for oxidation of VOCs (Y. , et al., 2005). Table 4.2 shows the plasma catalytic activity of Ag/TiO_2 catalyst. The results reveal that the presence of TiO_2 support affected the conversion by decreased the VOCs conversion from 95.3% to 83.4% which can be resulted from increasing in the resistance in plasma zone. Whereas the TiO_2-supported increased the CO_2 selectivity from 59% to 65% while the CO selectivity decreased from 31.3% to 29.4% when the TiO_2-supported was added. These results can be explained that TiO_2 could provide the high surface area for oxidation reaction and also could slow down CO radicals and CO molecules stayed longer in plasma zone that led to the opportunity of CO molecules to further oxidized with oxygen active species which can be converted to CO_2 as shown in CO_2 reaction formation ; $CO^{\bullet} + O^{\bullet} \rightarrow CO_2$.

In this study, the effects of various loadings of $0 - 5\%$ Ag on TiO_2 supports prepared by impregnation method were investigated for the VOCs conversion, CO and CO_2 selectivities. The operational conditions were kept at an applied voltage of 5 kV, an input frequency of 500 Hz, feed flow rate of 100 ml/min, an initial VOCs concentration in air of 100 ppm and electrodes gap distance of 15 mm.

The VOCs conversion increased with increasing the percentage of Ag loading from 0% to 1% Ag/TiO_2 and then tended to decrease with increasing the Ag loading to 5%. The highest VOCs conversion was observed at 1% Ag/TiO_2 which increased from 83.4% to 94.8% as compared to the TiO_2-supported. These results can be imply that the presence of proper amount of Ag metal on TiO_2-supported exhibited a good performance to the plasma catalytic process. However, increasing Ag loading directly decreased the surface area of catalyst led to decreased the VOCs conversion. The results are well correlated to the surface area shown in previous section.

When the percentage of Ag loading increased from 0% to 1% Ag/TiO_2, CO_2 selectivity increased whereas CO selectivity decreased. However, with further

increase Ag loading to 5%, the CO_2 selectivity decreased. The result shows that the 1% of Ag/TiO_2 played the significantly effect by decreasing the selectivity of CO from 29.4% to 14.5% and increasing the CO_2 selectivity from 65% to 78%. The decreasing of CO_2 selectivity due to the reason that high Ag loading reduced the surface area of catalysts corresponded to lowering oxidation reaction in plasma zone. Among six loadings of Ag on TiO_2 support, 1% Ag/TiO_2 is considered as the optimum condition in terms of high VOCs conversion of 94.8%, the high CO_2 selectivity of 78% and the lowest CO selectivity of 14.5%.

Table 4.2 The catalytic activity results of various Ag loading on TiO_2 support catalysts on VOCs conversion and product selectivity in this study

Catalyst	Loading (%)	VOCs conversion (%)	Selectivities (%)		
			CO	CO_2	CH_4
Sole Plasma	-	95.3	31.3	59.0	8.0
Ag/TiO_2	0	83.4	29.4	65.0	12.0
	0.5	90.2	24.8	75.0	7.0
	1	94.8	14.5	78.0	9.0
	2	85.8	21.8	71.0	10.0
	3	85.1	17.6	75.0	12.0
	4	89.1	16.9	74.0	9.0
	5	84.4	18.0	76.0	10.0

4.2.3 Effect of plasma catalytic activity testing on Ag/Al_2O_3 catalyst

Ag/Al_2O_3 catalyst has been widely studied for the oxidation of VOCs. However, rarely been studied for the complete oxidation of VOCs. Furthermore, silver is regarded as an environmentally friendly material. In this section, the effect of plasma catalytic activity testing using Al_2O_3-supported and Ag/Al_2O_3 on the VOCs conversion and the product selectivity were examined the Ag loading on Al_2O_3 supported were varied from 0% to 5% while other operational parameters were kept constant at an applied voltage of 5 kV, an input frequency of 500 Hz, feed flow rate of 100 ml/min, an initial VOCs concentration in air of 100 ppm and electrodes gap distance of 15 mm.

Table 4.3 illustrates the plasma catalytic activity of Ag/Al_2O_3 catalyst. The results display that in plasma environment, the presence of catalyst inside the plasma zone directly affects the plasma catalytic by increases the resistance of system. Therefore, the VOCs conversion decreased. As discussed in the characterization section, Al_2O_3-supported as well as Ag/Al_2O_3 had well dispersion even in high Ag loading (0% - 4%). In addition, large aggregates of Ag were not found when increased Ag loading (Figure 4.13). These results are well correlated to the small change of surface area of 154.3 m^2/g to 147.4 m^2/g when increased Ag loading from 1 to 4% Ag/Al_2O_3 respectively. Therefore, adding of Ag loading at a proper amount provided good enhancement for VOCs conversion.

The VOCs conversion increased when increased Ag loading from 0% - 4% Ag/Al_2O_3 and then slightly decreased when the Ag loading reached to 5% Ag/Al_2O_3. The highest VOCs conversion was observed at 4% Ag/Al_2O_3 catalyst by increasing from 86.9% to 97.1% as compared to the Al_2O_3-supported. In general, oxygen active species provided by plasma collision reactions will be randomly reacted with reactants to form various products. Since the 4% Ag/Al_2O_3 catalysts was added, the oxygen active species had opportunity to form Ag_2O which provided the further oxidation of CO to form CO_2.

When the Ag loadings increased from 0% to 4% Ag/Al_2O_3, the CO_2 selectivity increased whereas CO selectivity decreased. And then the CO_2

selectivity remain constant while increased the Ag loading to 5% Ag/Al_2O_3. The XPS results reveal that Ag_2O was reduced to metallic Ag during plasma catalytic reaction which were well correlated to explanation. The results illustrates that the presence of Ag metallic at a proper amount of 4% Ag/Al_2O_3 enhanced the plasma catalytic activity in terms of VOCs conversion and CO_2 selectivity.

Table 4.3 The catalytic activity results of various Ag loading on Al_2O_3 support catalysts on VOCs conversion and product selectivity in this study

Catalyst	Loading (%)	VOCs conversion (%)	Selectivities (%)		
			CO	CO_2	CH_4
Sole Plasma	-	95.3	31.3	59.0	8.0
Ag/Al₂O₃	0	86.9	25.6	70.0	10.0
	0.5	86.7	14.7	60.0	15.0
	1	90.0	16.1	79.0	10.0
	2	92.6	17.3	73.0	12.0
	3	93.1	11.3	78.5	10.0
	4	97.1	6.0	81.0	8.0
	5	96.9	14.8	80.0	10.0

4.2.1   <u>Effect of plasma catalytic activity testing on Mn/TiO_2 catalyst</u>

Mn/TiO_2 catalyst was considered as one of an active catalyst for the treatment of CO, NO_x, and VOCs due to the ability that has multivalent electrons, it can be formed in several stable oxides. Aforementioned about TiO_2-supported, in this study, the effects of various loadings of $0 - 5\%$ Mn on TiO_2 supports prepared by impregnation method were investigated for the VOCs conversion, CO and CO_2 selectivities. The operational conditions were kept at an applied voltage of 5 kV, an input frequency of 500 Hz, feed flow rate of 100 ml/min, an initial VOCs concentration in air of 100 ppm and electrodes gap distance of 15 mm.

Table 4.4 shows catalytic activity results of various Mn loading on TiO_2 support catalysts on VOCs conversion and product selectivity in this study. The VOCs conversion increased with increasing the percentage of Mn loading from 0% to 1% Mn/TiO_2 and then tended to decrease with increasing the Mn loading to 5%. The highest VOCs conversion was observed at 1% Mn/TiO_2 which increased from 83.4% to 88.4% as compared to the TiO_2-supported. The explanation for the decreasing in VOCs conversion when increased Mn loading from 1% to 5% Mn/TiO_2 is that the increasing in Mn loading decreased the surface area (Table 4.1) led to decrease the opportunity of high synergetic active species to collide with reactants.

When the Mn loading increased from 0% - 1% Mn/TiO_2, CO_2 selectivity increased whereas CO selectivity decreased. And then the CO_2 selectivity decreased when further increased to 5% Mn/TiO_2. The results indicated that the presence of Mn/TiO_2 affect the plasma catalytic activity by increasing the surface area allowing the oxygen active species to further oxidized with CO molecules to be converted to CO_2. The reason for the declined in catalytic activity when operated with 2% - 5% Mn/TiO_2 was mainly due to the increased in coke formation 0.5%, 14.25%, 10.3%, and 1.6% respectively.

Table 4.4 The catalytic activity results of various Mn loading on TiO_2 support
catalysts on VOCs conversion and product selectivity in this study

Catalyst	Loading (%)	VOCs conversion (%)	Selectivities (%)		
			CO	CO_2	CH_4
Sole Plasma	-	95.3	31.3	59.0	8.0
Mn/TiO$_2$	0	83.4	29.4	65.0	12.0
	0.5	88.3	16.5	65.0	9.0
	1	88.4	19.9	74.0	10.0
	2	73.0	18.5	69.0	12.0
	3	67.7	21.8	52.0	12.0
	4	77.6	17.7	61.5	10.5
	5	84.9	12.9	75.0	8.5

From Table 4.4 also represented the result of the effect of the percentage of Mn loading on TiO_2 support on CO and CO_2 selectivities. When the percentage of Mn loadings increased to 1% Mn/TiO$_2$, CO_2 selectivity increased whereas CO selectivity decreased. And then the CO_2 selectivity decreased when increased the percentage of Mn loading. The result showed that the 1% of Mn/TiO$_2$ played the significantly effect by decreasing the selectivity of CO from 29.4% to 19.9% and increase the CO_2 selectivity from 65% to 74%. When further increases the percentage of Mn loading, the coke formation was occurred in the reactor then leaded to the summarize that among six loadings of Mn on TiO_2 support, 1% Mn/TiO$_2$ is the best choice in terms of the highest VOCs conversion at 88.4%, high CO_2 selectivity at 74%, low CO selectivity at 14.5% with no coke formation.

4.2.2 Effect of plasma catalytic activity testing on Mn/Al$_2$O$_3$ catalyst

Aforementioned about Al$_2$O$_3$ support, In this section, the effect of plasma catalytic activity testing using Al$_2$O$_3$-supported and Mn/Al$_2$O$_3$ on the VOCs conversion and the product selectivity were examined the Mn loading on Al$_2$O$_3$ supported were varied from 0% to 5% while other operational parameters were kept constant at an applied voltage of 5 kV, an input frequency of 500 Hz, feed flow rate of 100 ml/min, an initial VOCs concentration in air of 100 ppm and electrodes gap distance of 15 mm.

Table 4.5 illustrates the plasma catalytic activity of Mn/Al$_2$O$_3$ catalyst. The results display that in plasma environment, the presence of catalyst inside the plasma zone directly affects the plasma catalytic by increases the resistance of system. Therefore, the VOCs conversion decreased. As discussed in the characterization section, Al$_2$O$_3$-supported as well as Mn/Al$_2$O$_3$ had well dispersion even in high Mn loading (0% - 5%). In addition, large aggregates of Mn were not found when increased Mn loading (Figure 4.15). These results are well correlated to the small change of surface area of 155.2 m^2/g to 152.5 m^2/g when increased Mn loading from 1 to 5% Mn/Al$_2$O$_3$ respectively. Therefore, adding of Mn loading at a proper amount provided good enhancement for VOCs conversion.

The VOCs conversion increased when increased Mn loading from 0% - 5% Mn/Al$_2$O$_3$. The highest VOCs conversion was observed at 5% Mn/Al$_2$O$_3$ catalyst which increased from 86.9% to 95.0% as compared to the Al$_2$O$_3$-supported. The increased in Mn loading not only affected changing the surface area but also increased the Mn oxides (MnO, MnO$_2$, and Mn$_2$O$_3$,) which led to enhance the opportunity of collision between active species.

When the Mn loading increased from 0% - 5% Mn/Al$_2$O$_3$, CO$_2$ selectivity increased whereas CO selectivity decreased. The results indicated that the presence of Mn/TiO$_2$ affect the plasma catalytic activity by increasing the surface area allowing the oxygen active species to further oxidized with CO molecules to be converted to CO$_2$.

Table 4.5 The catalytic activity results of various Mn loading on Al_2O_3 support catalysts on VOCs conversion and product selectivity in this study

Catalyst	Loading (%)	VOCs conversion (%)	Selectivities (%)		
			CO	CO_2	CH_4
Sole Plasma	-	95.3	31.3	59.0	8.0
Mn/Al$_2$O$_3$	0	86.9	25.6	70.0	10.0
	0.5	82.4	16.7	76.0	11.0
	1	78.1	25.8	62.0	11.5
	2	71.8	19.8	63.0	11.5
	3	80.9	16.1	70.5	10.5
	4	82.4	15.5	71.0	9.5
	5	95.0	14.7	77.0	9.0

Table 4.6 shows plasma catalytic activity of selected catalysts at their own optimum loading which corresponding to the highest VOCs conversion and CO_2 selectivity. The results reveal that the addition of catalysts could enhance the VOCs decomposition performance in terms of increasing CO_2 selectivity and decreasing CO selectivity. The reason is that plasma catalytic process provided an opportunity for oxygen active species (oxygen radicals and metal oxide radicals) to further oxidized with CO molecules to be converted to CO_2.

Focusing on the two different supports, Al_2O_3-supported exhibited a better performance in both Ag and Mn metal as compared to the TiO_2-supported. The SEM image shows a good distribution of Ag and Mn particles on Al_2O_3 support as shown in Figure 4.13 and Figure 4.15. Comparison between Ag and Mn metal on both supports, Ag metal provided higher CO_2 selectivity as compared to the Mn metal. As explained in characterization section, the existence of Ag_2O of the loaded Ag on both TiO_2 and Al_2O_3 before plasma catalytic reaction were verified by the deconvoluted XPS spectra while after reaction only Ag metallic observed as shown

in Figure 4.18 and Figure 4.19. The XPS spectra results suggest that Ag_2O was reduced to metallic Ag during plasma catalytic reaction.

Table 4.6 Plasma catalytic activity of selected catalysts at their own optimum loading (corresponding to the highest VOCs conversion and CO_2 selectivity)

Catalyst	Loading (%)	VOCs conversion (%)	Selectivities (%)		
			CO	CO_2	CH_4
Sole Plasma	-	95.3	31.3	59.0	8.0
Ag/TiO$_2$	1	94.8	14.5	78.0	9.0
Ag/Al$_2$O$_3$	4	97.1	6.0	81.0	8.0
Mn/TiO$_2$	1	88.4	19.9	74.0	10.0
Mn/Al$_2$O$_3$	5	95.0	14.7	77.0	9.0

For the loaded Mn on both TiO_2 and Al_2O_3 supports, fresh catalysts shown various forms of Mn oxide (MnO, MnO_2, and Mn_2O_3). However, Mn metal peak was not observed in spent catalysts. These results can be imply that oxygen active species provided by plasma process prefer to oxidize with Mn oxide led to change their oxidation state more than oxidize with CO radical. Among various catalysts, 4% Ag/Al$_2$O$_3$ was selected to be the best catalysts for VOCs decomposition using plasma catalytic process in terms of providing the highest VOCs conversion and CO_2 selectivity and the lowest CO selectivity.

CHAPTER V
CONCLUSIONS AND RECOMMENDATIONS

5.1 Conclusions

In this study, Silver (Ag) and Manganese (Mn) catalysts loaded on TiO_2 and Al_2O_3 support on quartz wool were tested for the removal of mixed VOCs of benzene, toluene, and xylene by using catalytic corona discharge in nonthermal plasma system. The optimum condition for a single stage corona discharge were found at an applied voltage of 5 kV, input frequency of 500 Hz, feed flow rate of 100.0 ml/min, and the gap distance between electrodes of 15mm. Under these optimum conditions, the VOCs conversion and CO_2 selectivity were found to be 95.3 and 59.0 %, respectively.

For the effect of the presence of catalysts, among all various Ag and Mn loading on TiO_2 and Al_2O_3 support catalysts, the presence of 1% Ag/TiO_2, 4% Ag/Al_2O_3, 1% Mn/TiO_2 and 5% Mn/Al_2O_3 catalysts in the pin and plate corona discharge reactor was found to improve the CO_2 selectivity from 59% to 78.0%, 81.0%, 74.0% and 77.0% respectively while the CO selectivity was reduced from 31.3% to 14.5%, 6.0%, 19.9% and 15.5% respectively.

5.2 Recommendations

1. To do the multistage of catalytic corona discharge system for achieve 100% carbon dioxide selectivity.

2. To develop the bi-metallic oxide catalysts for more conversion and the higher selectivity of CO_2.

REFERENCES

Begerow, J., Jermann, E., Keles, T., Koch, T., & Dunemann, L. (1996). Screen method for the determination of 28 volatile organic compounds in indoor and outdoor air at environmental concentrations using dual-column capillary gas chromatography with tandem electron-capture-flame ionization detection. *Journal of Chromatography A*, 181-191.

Chang, J.-S. (2001). Recent development of plasma pollution control. *Science and Technology of Advanced Materials*, 571-576.

Chang, J.-S., Lawless, P. A., & Yamamoto, T. (1991). Corona Discharge Processes. *IEEE TRANSACTIONS ON PLASMA SCIENCE*, 1151-1166.

Chang, J.-S., Phill, A., Lawless, & Yamamoto, T. (1991). Corona Discharge Processes. *TRANSACTIONS ON PLASMA SCIENCE*, 1152-1166.

Chavadej, S., Kiatubolpaiboon, W., Rangsunvigit, P., & Sreethawong, T. (2007). A combined multistage corona discharge and catalytic system for gaseous benzene removal. *Journal of Molecular Catalysis A : Chemical*, 128-136.

Chongterdtoonskul, A., Schwank, J. W., & Chavadej, S. (2013). Comparative study on the influence of second metals on Ag-loaded mesoporous. *Journal of Molecular Catalysis A: Chemical*, 175-182.

Conrads, H., & Schmidt, M. (2000). Plasma generation and plasma sources. *Plasma sources science and technology*, 441-454.

Dendy, R. O. (1990). *Plasma Dynamics*. Oxford: Oxford science.

Durme, J. V., Dewulf, J., Leys, C., & Langenhove, H. V. (2008). Combining non-thermal plasma with heterogeneous catalysis. *Applied Catalysis*, 324-333.

Elfadly, A., Zeid, I., Yehia, F., Rabie, A., aboualala, M., & Park, S.-E. (2016). Highly selective BTX from catalyticfast pyrolysis of lignin over supported mesoporous silica. *International Journal of Biological Macromolecules*, 278-293.

Eliasson, B., Hirth, M., & Kogelschatz, U. (1987). Ozone synthesis from oxygen in dielectric barrier discharges. *Journal of Physics D: Applied Physics*.

Guo, Y., Liao, X., He, J., Ou, W., & Ye, D. (2010). Effects of manganese oxide catalyst on dielectric barrier discharge decomposition of toluene. *Catalysis today*, 176-183.

Hippler, R., Kerste, H., Schmidt, M., & Schoenbach, K. H. (2007). *Low Temperature Plasmas* . WILEY-VCH Verlag GmbH & Co. KGaA .

Kanjanasiranont, N., Prueksasit, T., & Morknoy, D. (2017). Inhalation exposure and health risk levels to BTEX and carbonyl. *Atmospheric Environment*, 111-120.

Keidar, M., & Beilis, I. I. (2013). *Plasma Engineering application from aerospace to bio and nanotechnology* . San Diego: Elsevier.

Kim, H.-H., Kobara, H., Ogata, A., & Futamura, S. (2005). Comparative Assessment of Different Nonthermal. *IEEEE TRANSACTIONS ON INDUSTRY APPLICATIONS*, 206-214.

Kizling, B. M., & Sven , G. (1996). A review of the use of plasma techniques in catalyst. *Applied Catalysis*, 1-21.

Kogelschatz, U. (2003). Dielectric-barrier Discharges: Their History,. *Plasma Chemistry and Plasma Processing*, 1-46.

Lee, B.-Y., Park, S.-H., Lee, S.-C., Kang, M., & Choung, S.-J. (2004). Decomposition of benzene by using a discharge plasma-photocatalyst hybrid system. *Catalysis Today*, 769-776.

Li, D., Yakushiji, D., Kanazawa, S., Ohkubo, T., & Nomoto, Y. (2002). Decomposition of toluene by streamer corona discharge with catalyst. *Journal of Electrostatics*, 311-319.

Liotta, L. (2010). Review Catalytic oxidation of volatile organic compounds on supported noble metals. *Applied Catalysis B: Environmental*, 403-412.

Ogata, A., Shintani, N., Yamanouchi, K., Mizuno, K., Kushiyama, S., & Yamamoto, T. (2000). Effect of Water Vapor on Benzene Decomposition. *Plasma Chemistry and Plasma Processing*, 453-467.

Ongwandee, M., & Chavalparit, O. (2010). Commuter exposure to BTEX in public transportation modes. *Journal of Environmental Sciences*, 397-404.

Parvulescu, V. I., Magureanu, M., & Lukes, P. (2012). *Plasma Chemistry and Catalyst in Gases and Liquids.* Weinheim, Germany: Deutsche Nationalbibliothek.

Paulmier, T., & Fulcheri, L. (2005). Use of non-thermal plasma for hydrocarbon reforming. *Chemical Engineering Journal*, 59-71.

S., I., Y., T., M., M., & T., I. (1995). Cooperative Action of Palladium and Manganese(III) Oxide in the Oxidation of Carbon Monoxide. *Journal of Catalysis*, 279-284.

Sano, T., Negishi, N., Sakai, E., & Matsuzawa, S. (2006). Contributions of photocatalytic/catalytic activities of TiO2 and gamma-Al2O3 in nonthermal plasma on oxidation of acetaldehyde and CO. *Journal of Molecular Catalysis A : Chemical*, 235-241.

Song, Y.-H., Kim, S.-J., Choi, K.-I., & Yamamoto, T. (2002). Effects of adsorption and temperature on a nonthermal plasma process for removing VPCs. *Journal of Electrostatics*, 189-201.

Strohmeier, B. R. (1995). GammaAlumina (Al2O3) by XPS. *Surface Science Spectra* , 135-140.

Subrahmanyam, C., Renken, A., & Kiwi-Minsker, L. (2007). Novel catalytic non-thermal plasma reactor for the abatement of VOCs. *Chemical Engineering Journal*, 78-83.

Urashima, K., & Chang, J.-S. (2000). Removal of Volatile Organic Compounds. *Transactions on Dielectrics and Electrical Insulation*, 602-614.

Urashima, K., & Chang, J.-S. (2000). Removal of Volatile Organic Compounds from Air Streams and Industrial Flue Gases by Non-Thermal Plasma Technology. *IEEE Treansactions on Dielectrics and Electrical Insulation*, 602-614.

Vandenbroucke, A. M., Morent, R., Geyter, N. D., & Leys, C. (2011). Non-thermal plasmas for non-catalytic and catalytic VOC abatement. *Journal of Hazardous Materials* , 30-54.

Xu, X. (2001). *Thin Solid Films*, 237-242.

Xu, X. (2001). Dielectric barrier discharge - properties and applications. *Thin Solid Films*, 237-242.

Y. , M., J. , S., I., K., K. , T., S. , K., & A., M. (2005). After-Treatment of NOX Using Combination of Non-Thermal Plasma. *J. Adv. Oxid. Technol*.

APPENDICES

APPENDIX A EXPERIMENTAL DATA

Table A.1 Effect of applied voltage on VOCs conv

Table A.2ersion and CO and CO_2 selectivity of the studied input frequency of 400, 450, and 500 Hz, an initial VOCs concentration of 100 ppm, total feed flow rate of 100.0 ml/min, and the gap distance between pin and plate electrode of 15 mm

Applied Voltage (kV)	Parameters	Input Frequency (Hz)		
		400	450	500
5	Benzene Conversion (%)	93.7	95.4	93.4
	Toluene Conversion (%)	96.8	97.6	95.5
	Xylene Conversion (%)	98.4	99.0	97.7
	VOCs Conversion (%)	96.1	97.2	95.3
	CO_2 Selectivity (%)	63.6	74.3	59.0
	CO Selectivity (%)	18.7	24.4	31.3
	CH_4 Selectivity (%)	9.0	9.0	8.0
	Carbon balance (%)	-8.7	7.7	-1.7
	Current (mA)	140.0	80.0	70.0
6	Benzene Conversion (%)	96.1	95.7	93.7
	Toluene Conversion (%)	97.9	97.6	96.6
	Xylene Conversion (%)	99.1	98.8	98.1
	VOCs Conversion (%)	97.6	97.3	95.9
	CO_2 Selectivity (%)	67.8	75.3	64.0
	CO Selectivity (%)	21.6	16.8	28.0
	CH_4 Selectivity (%)	8.0	8.0	9.0
	Carbon balance (%)	-2.6	0.0	1.0
	Current (mA)	90.0	90.0	80.0

Applied Voltage (kV)	Parameters	Input Frequency (Hz)		
		400	450	500
7	Benzene Conversion (%)	96.6	95.6	94.8
	Toluene Conversion (%)	98.2	97.8	96.9
	Xylene Conversion (%)	99.1	99.1	98.3
	VOCs Conversion (%)	97.9	97.4	96.5
	CO_2 Selectivity (%)	68.0	78.1	77.0
	CO Selectivity (%)	21.4	14.4	15.2
	CH_4 Selectivity (%)	8.0	9.0	9.0
	Carbon balance (%)	-2.6	1.5	1.2
	Current (mA)	110.0	110.0	90.0
8	Benzene Conversion (%)	97.1	95.8	95.3
	Toluene Conversion (%)	98.5	97.8	97.2
	Xylene Conversion (%)	99.6	99.1	98.7
	VOCs Conversion (%)	98.1	97.4	96.8
	CO_2 Selectivity (%)	74.1	79.7	78.0
	CO Selectivity (%)	15.1	9.0	15.6
	CH_4 Selectivity (%)	8.0	8.0	9.0
	Carbon balance (%)	-2.8	-3.2	2.6
	Current (mA)	120.0	120.0	100.0
9	Benzene Conversion (%)	96.7	96.1	95.8
	Toluene Conversion (%)	98.5	97.9	97.8
	Xylene Conversion (%)	99.7	99.2	99.2
	VOCs Conversion (%)	98.2	97.6	97.5
	CO_2 Selectivity (%)	78.7	80.1	81.0
	CO Selectivity (%)	14.5	14.0	9.1
	CH_4 Selectivity (%)	8.0	9.0	9.0
	Carbon balance (%)	1.2	3.1	-1.0
	Current (mA)	140.0	130.0	120.0

Applied Voltage (kV)	Parameters	Input Frequency (Hz)		
		400	450	500
10	Benzene Conversion (%)	96.7	96.2	95.9
	Toluene Conversion (%)	98.5	97.9	97.6
	Xylene Conversion (%)	99.6	99.2	98.9
	VOCs Conversion (%)	98.3	97.6	97.4
	CO_2 Selectivity (%)	79.1	82.9	80.0
	CO Selectivity (%)	11.3	7.3	7.9
	CH_4 Selectivity (%)	7.0	9.0	9.0
	Carbon balance (%)	-2.6	-0.8	-3.1
	Current (mA)	160.0	150.0	130.0

Table A.3 Effect of applied voltage on VOCs conversion and CO and CO_2 selectivity of the studied applied voltage of 5, 6, 7, 8, 9, and 10 kV at an initial VOCs concentration of 100 ppm, total feed flow rate of 100.0 ml/min, and the gap distance between pin and plate electrode of 15 mm

Input Frequency (Hz)	Parameters	Applied Voltage (kV)					
		5	6	7	8	9	10
400	Benzene Conversion (%)	93.7	96.1	96.6	97.1	96.7	96.7
	Toluene Conversion (%)	96.8	97.9	98.2	98.5	98.5	98.5
	Xylene Conversion (%)	98.4	99.1	99.1	99.6	99.7	99.6
	VOCs Conversion (%)	96.1	97.6	97.9	98.1	98.2	98.3
	CO_2 Selectivity (%)	63.6	67.8	68.0	74.1	78.7	79.1
	CO Selectivity (%)	18.7	21.6	21.4	15.1	14.5	11.3
	CH_4 Selectivity (%)	9.0	8.0	8.0	8.0	8.0	7.0
	Carbon balance (%)	-8.7	-2.6	-2.6	-2.8	1.2	-2.6
	Current (mA)	140.0	90.0	110.0	120.0	140.0	160.0

Input Frequency (Hz)	Parameters	Applied Voltage (kV)					
		5	6	7	8	9	10
450	Benzene Conversion (%)	95.4	95.7	95.6	95.8	96.1	96.2
	Toluene Conversion (%)	97.6	97.6	97.8	97.8	97.9	97.9
	Xylene Conversion (%)	99.0	98.8	99.1	99.1	99.2	99.2
	VOCs Conversion (%)	97.2	97.3	97.4	97.4	97.6	97.6
	CO_2 Selectivity (%)	74.3	75.3	78.1	79.7	80.1	82.9
	CO Selectivity (%)	24.4	16.8	14.4	9.0	14.0	7.3
	CH_4 Selectivity (%)	9.0	8.0	9.0	8.0	9.0	9.0
	Carbon balance (%)	7.7	0.0	1.5	-3.2	3.1	-0.8
	Current (mA)	80.0	90.0	110.0	120.0	130.0	150.0
500	Benzene Conversion (%)	93.4	93.7	94.8	95.3	95.8	95.9
	Toluene Conversion (%)	95.5	96.6	96.9	97.2	97.8	97.6
	Xylene Conversion (%)	97.7	98.1	98.3	98.7	99.2	98.9
	VOCs Conversion (%)	95.3	95.9	96.5	96.8	97.5	97.4
	CO_2 Selectivity (%)	59.0	64.0	77.0	78.0	81.0	80.0
	CO Selectivity (%)	31.3	28.0	15.2	15.6	9.1	7.9
	CH_4 Selectivity (%)	8.0	9.0	9.0	9.0	9.0	9.0
	Carbon balance (%)	-1.7	1.0	1.2	2.6	-1.0	-3.1
	Current (mA)	70.0	80.0	90.0	100.0	120.0	130.0

Table A.4 Effect of the presence of catalysts on VOCs conversion and CO and CO_2 selectivity of the studied catalysts at an initial VOCs concentration of 100 ppm, total feed flow rate of 100.0 ml/min, and the gap distance between pin and plate electrode of 15 mm

Catalyst	Loading (%)	VOCs conversion (%)	Selectivities (%)			Carbon Balance (%)
			CO	CO_2	CH_4	
Sole Plasma System	-	95.3	31.3	59.0	8.0	-1.7
TiO_2	-	83.4	29.4	65.0	12.0	6.4
Al_2O_3	-	86.9	25.6	70.0	10.0	5.6
Ag/TiO_2	0	83.4	29.4	65.0	12.0	6.4
	0.5	90.2	24.8	75.0	7.0	6.8
	1	94.8	14.5	78.0	9.0	1.5
	2	85.8	21.8	71.0	10.0	2.8
	3	85.1	17.6	78.0	12.0	7.6
	4	89.1	16.9	74.0	9.0	-0.1
	5	84.4	18.0	76.0	10.0	4.0
Ag/Al_2O_3	0	86.9	25.6	70.0	10.0	5.6
	0.5	86.7	14.7	60.0	15.0	-10.3
	1	90.0	16.1	79.0	10.0	5.1
	2	92.6	17.3	73.0	12.0	2.3
	3	94.1	11.5	79.0	10.0	0.5
	4	97.1	6.0	81.0	8.0	-5.0
	5	96.9	14.8	80.0	10.0	4.8

Catalyst	Loading (%)	VOCs conversion (%)	Selectivities (%)			Carbon Balance (%)
			CO	CO_2	CH_4	
Mn/TiO$_2$	0	83.4	29.4	65.0	12.0	6.4
	0.5	88.3	16.5	65.0	9.0	-9.5
	1	88.4	19.9	74.0	10.0	3.9
	2	73.0	18.5	69.0	12.0	-0.5
	3	67.7	21.8	52.0	12.0	-14.2
	4	77.6	17.7	61.5	10.5	-10.3
	5	84.9	12.9	75.0	8.5	-3.6
Mn/Al$_2$O$_3$	0	86.9	25.6	70.0	10.0	5.6
	0.5	82.4	16.7	76.0	11.0	3.7
	1	78.1	25.8	62.0	11.5	-0.7
	2	71.8	19.8	63.0	11.5	-5.7
	3	80.9	16.1	70.5	10.5	-2.9
	4	84.4	14.7	71.0	9.5	-4.8
	5	95.0	15.5	77.0	9.0	1.5

Table A.5 Products information from GC-MS analysis

Name	Formula	Retention time (s)	Area	Height
Formic acid	CH_2O_2	307.20	2087064	6.13
Acetic acid	$C_2H_4O_2$	319.60	15928690	46.82
Ethanol, 2-nitro-, propionate (ester)	$C_5H_9NO_4$	342.10	104248	0.31
2-Propenoic acid	$C_3H_4O_2$	344.50	232668	0.68
Acetic anhydride	$C_4H_6O_3$	364.70	1051713	3.09
$CH_3C(O)CH_2CH_2OH$	$C_4H_8O_2$	470.65	548540	1.61
Furfural	$C_5H_4O_2$	508.60	143486	0.42
2-Cyclopenten-1-one	C_5H_6O	526.30	309961	0.91
Cyclopent-4-ene-1,3-dione	$C_5H_4O_2$	660.15	439221	1.29
4-Cyclopentene-1,3-dione	$C_5H_4O_2$	672.90	639934	1.88
3,4 Epoxytetrahydro-thiophene-1,1-dioxide	C4H6O3S	684.05	66955	0.20
Phenol	C6H6O	688.90	358795	1.05
p-Benzoquinone	C6H4O2	706.50	1073177	3.15
Benzaldehyde	C7H6O	710.75	3819624	11.23
2(5H)-Furanone	C4H4O2	746.75	303429	0.89
2H-Pyran-2-one	C5H4O2	820.40	176778	0.52
Benzyl alcohol	C7H8O	831.40	2035866	5.98
1,4-Cyclohex-2-enedione	C6H6O2	931.15	120936	0.36
3-Methylbenzyl alcohol	C8H10O	1000.55	650300	1.91
Isophthalaldehyde	C8H6O2	1314.40	143485	0.42

Table A.6 Effect of applied voltage on VOCs conversion and CO and CO_2 selectivity in terms of concentration inlet and concentration outlet (ppm) on sole plasma which the studied input frequency of 400, 450, and 500 Hz, an initial VOCs concentration of 100 ppm, total feed flow rate of 100.0 ml/min, and the gap distance between pin and plate electrode of 15 mm

Applied Voltage (kV)	Input Frequency (Hz)	Catalyst	Parameters	Conversion /Selectivity (%)	Outlet Concentration (ppm)
5	400	Sole plasma	VOCs	96.10	3.23
			Benzene	93.70	1.80
			Toluene	96.80	0.95
			Xylene	98.40	0.48
			CO	18.70	33.99
			CO_2	63.60	183.04
			CH_4	9.00	9.39
6	400	Sole plasma	VOCs	97.60	2.22
			Benzene	96.10	1.24
			Toluene	97.90	0.67
			Xylene	99.10	0.31
			CO	21.60	43.53
			CO_2	67.80	214.61
			CH_4	8.00	8.67
7	400	Sole plasma	VOCs	97.90	1.73
			Benzene	96.60	0.95
			Toluene	98.20	0.50
			Xylene	99.10	0.27
			CO	21.40	25.94
			CO_2	68.00	220.89
			CH_4	8.00	8.51
8	400	Sole plasma	VOCs	98.10	1.45
			Benzene	97.10	0.88
			Toluene	98.50	0.44
			Xylene	99.60	0.13
			CO	15.10	28.62
			CO_2	74.10	220.94
			CH_4	8.00	8.44

Applied Voltage (kV)	Input Frequency (Hz)	Catalyst	Parameters	Conversion/ Selectivity (%)	Outlet Concentration (ppm)
9	400	Sole plasma	VOCs	98.20	2.27
			Benzene	96.70	0.91
			Toluene	98.50	0.43
			Xylene	99.70	0.94
			CO	14.50	20.11
			CO_2	78.70	220.43
			CH_4	8.00	8.54
10	400	Sole plasma	VOCs	98.30	1.68
			Benzene	96.70	1.07
			Toluene	98.50	0.48
			Xylene	99.60	0.12
			CO	11.30	44.05
			CO_2	79.10	219.42
			CH_4	7.00	8.59
5	450	Sole plasma	VOCs	97.20	2.07
			Benzene	95.40	1.18
			Toluene	97.60	0.62
			Xylene	99.00	0.28
			CO	24.40	42.84
			CO_2	74.30	204.91
			CH_4	9.00	8.65
6	450	Sole plasma	VOCs	97.30	2.00
			Benzene	95.70	1.12
			Toluene	97.60	0.63
			Xylene	98.80	0.25
			CO	16.80	16.52
			CO_2	75.30	229.06
			CH_4	8.00	8.80
7	450	Sole plasma	VOCs	97.40	2.11
			Benzene	95.60	1.20
			Toluene	97.80	0.64
			Xylene	99.10	0.27
			CO	14.40	23.35
			CO_2	78.10	209.52
			CH_4	9.00	8.86

Applied Voltage (kV)	Input Frequency (Hz)	Catalyst	Parameters	Conversion /Selectivity (%)	Outlet Concentration (ppm)
8	450	Sole plasma	VOCs	97.40	1.94
			Benzene	95.80	1.09
			Toluene	97.80	0.61
			Xylene	99.10	0.24
			CO	9.00	15.98
			CO_2	79.90	221.58
			CH_4	8.00	8.52
9	450	Sole plasma	VOCs	97.60	1.84
			Benzene	96.10	1.03
			Toluene	97.90	0.59
			Xylene	99.20	0.22
			CO	14.00	12.47
			CO_2	80.10	224.19
			CH_4	9.00	8.61
10	450	Sole plasma	VOCs	97.60	2.03
			Benzene	96.20	1.16
			Toluene	97.90	0.63
			Xylene	99.20	0.24
			CO	7.30	24.87
			CO_2	82.90	212.43
			CH_4	9.00	8.67
5	500	Sole plasma	VOCs	95.30	4.53
			Benzene	93.40	2.24
			Toluene	95.50	1.54
			Xylene	97.70	0.75
			CO	31.30	63.74
			CO_2	59.00	188.44
			CH_4	8.00	9.84
6	500	Sole plasma	VOCs	95.90	3.47
			Benzene	93.70	1.88
			Toluene	96.60	1.03
			Xylene	98.10	0.57
			CO	16.80	51.34
			CO_2	75.30	183.20
			CH_4	8.00	9.71

Applied Voltage (kV)	Input Frequency (Hz)	Catalyst	Parameters	Conversion /Selectivity (%)	Outlet Concentration (ppm)
7	500	Sole plasma	VOCs	96.50	2.81
			Benzene	94.80	1.49
			Toluene	96.90	0.85
			Xylene	98.30	0.47
			CO	15.20	26.17
			CO_2	77.00	207.55
			CH_4	9.00	8.65
8	500	Sole plasma	VOCs	96.80	2.58
			Benzene	95.30	1.38
			Toluene	97.20	0.83
			Xylene	98.70	0.37
			CO	15.60	27.79
			CO_2	78.00	217.77
			CH_4	9.00	8.76
9	500	Sole plasma	VOCs	97.50	1.96
			Benzene	95.80	1.11
			Toluene	97.80	0.62
			Xylene	99.20	0.23
			CO	9.10	15.60
			CO_2	81.00	219.80
			CH_4	9.00	8.78
10	500	Sole plasma	VOCs	97.40	1.96
			Benzene	95.90	1.02
			Toluene	97.60	0.63
			Xylene	98.90	0.30
			CO	7.90	13.02
			CO_2	80.00	205.16
			CH_4	9.00	8.44

Table A.7 Effect of applied voltage on VOCs conversion and CO and CO_2 selectivity in terms of concentration inlet and concentration outlet (ppm) on studied catalysts at an initial VOCs concentration of 100 ppm, total feed flow rate of 100.0 ml/min, the electrode gap distance of 15 mm, an applied voltage of 5 kV and input frequency of 100 ml/min.

Catalyst	Parameters	Conversion /Selectivity (%)	Outlet Concentration (ppm)
TiO$_2$	VOCs	83.40	13.91
	Benzene	75.59	6.16
	Toluene	85.03	4.52
	Xylene	88.77	3.23
	CO	29.40	45.57
	CO$_2$	65.00	159.38
	CH$_4$	12.00	10.25
Al$_2$O$_3$	VOCs	86.90	10.93
	Benzene	82.30	5.09
	Toluene	87.80	3.45
	Xylene	91.84	2.39
	CO	25.60	41.18
	CO$_2$	70.00	176.55
	CH$_4$	10.00	9.49
0.5% Ag/TiO$_2$	VOCs	90.20	8.88
	Benzene	87.77	3.77
	Toluene	90.64	2.87
	Xylene	92.87	2.24
	CO	24.80	44.41
	CO$_2$	75.00	209.97
	CH$_4$	9.00	8.72
1% AgTiO$_2$	VOCs	94.80	4.22
	Benzene	93.07	1.97
	Toluene	95.47	1.29
	Xylene	96.59	0.96
	CO	14.50	25.03
	CO$_2$	78.00	209.97
	CH$_4$	9.00	9.16

Catalyst	Parameters	Conversion /Selectivity (%)	Outlet Concentration (ppm)
2% Ag/TiO$_2$	VOCs	85.80	11.92
	Benzene	81.42	5.40
	Toluene	88.18	3.46
	Xylene	89.17	3.06
	CO	21.80	34.75
	CO$_2$	71.00	177.75
	CH$_4$	10.00	9.38
3% Ag/TiO$_2$	VOCs	85.10	12.71
	Benzene	84.88	4.89
	Toluene	87.38	4.10
	Xylene	88.42	3.72
	CO	17.60	26.37
	CO$_2$	78.00	169.21
	CH$_4$	15.00	31.23
4% Ag/TiO$_2$	VOCs	89.10	9.21
	Benzene	79.45	6.19
	Toluene	93.63	1.94
	Xylene	96.54	1.08
	CO	16.90	29.83
	CO$_2$	74.00	203.40
	CH$_4$	9.00	8.60
5% Ag/TiO$_2$	VOCs	84.40	11.66
	Benzene	63.83	9.94
	Toluene	95.32	1.31
	Xylene	98.61	0.41
	CO	18.00	28.07
	CO$_2$	76.00	185.47
	CH$_4$	10.00	8.77
0.5% Ag/Al$_2$O$_3$	VOCs	86.70	12.64
	Benzene	79.22	6.10
	Toluene	86.19	4.05
	Xylene	91.71	2.49
	CO	14.70	28.49
	CO$_2$	60.00	197.63
	CH$_4$	9.00	9.35

Catalyst	Parameters	Conversion /Selectivity (%)	Outlet Concentration (ppm)
1% Ag/Al$_2$O$_3$	VOCs	90.00	7.69
	Benzene	82.64	5.39
	Toluene	94.43	1.74
	Xylene	97.29	0.56
	CO	16.10	25.86
	CO$_2$	79.00	200.53
	CH$_4$	10.00	8.85
2% Ag/Al$_2$O$_3$	VOCs	92.60	4.76
	Benzene	90.83	2.18
	Toluene	94.23	1.29
	Xylene	93.37	1.29
	CO	17.30	22.44
	CO$_2$	73.00	148.15
	CH$_4$	12.00	8.61
3% Ag/Al$_2$O$_3$	VOCs	94.10	4.95
	Benzene	90.69	3.33
	Toluene	95.47	1.12
	Xylene	97.36	0.51
	CO	11.50	17.28
	CO$_2$	79.00	188.43
	CH$_4$	10.00	8.55
4% Ag/Al$_2$O$_3$	VOCs	97.10	2.30
	Benzene	94.42	1.66
	Toluene	98.32	0.49
	Xylene	99.47	0.15
	CO	6.00	10.85
	CO$_2$	81.00	231.40
	CH$_4$	8.00	8.46
5% Ag/Al$_2$O$_3$	VOCs	96.90	2.41
	Benzene	93.77	1.82
	Toluene	98.33	0.47
	Xylene	99.59	0.12
	CO	14.80	26.79
	CO$_2$	80.00	227.01
	CH$_4$	10.00	8.44

Catalyst	Parameters	Conversion /Selectivity (%)	Outlet Concentration (ppm)
0.5% Mn/TiO$_2$	VOCs	88.30	15.77
	Benzene	78.68	6.80
	Toluene	83.67	5.24
	Xylene	88.40	3.73
	CO	29.40	31.51
	CO$_2$	65.00	156.50
	CH$_4$	12.00	9.09
1% Mn/TiO$_2$	VOCs	88.40	9.05
	Benzene	84.63	4.03
	Toluene	88.15	3.14
	Xylene	93.40	1.88
	CO	19.90	30.60
	CO$_2$	74.00	178.64
	CH$_4$	10.00	8.86
2% Mn/TiO$_2$	VOCs	73.00	20.70
	Benzene	68.04	9.05
	Toluene	71.05	8.28
	Xylene	78.92	3.36
	CO	18.50	24.70
	CO$_2$	69.00	151.46
	CH$_4$	12.00	8.94
3% Mn/TiO$_2$	VOCs	67.70	36.07
	Benzene	60.51	13.21
	Toluene	66.51	11.80
	Xylene	68.52	11.07
	CO	21.80	28.35
	CO$_2$	52.00	99.46
	CH$_4$	12.00	9.43
4% Mn/TiO$_2$	VOCs	77.60	29.98
	Benzene	75.79	13.72
	Toluene	78.83	9.42
	Xylene	79.57	6.84
	CO	17.70	27.58
	CO$_2$	61.50	108.64
	CH$_4$	10.50	9.29

Catalyst	Parameters	Conversion /Selectivity (%)	Outlet Concentration (ppm)
5% Mn/TiO$_2$	VOCs	84.90	2.21
	Benzene	82.26	1.30
	Toluene	87.73	0.65
	Xylene	89.15	0.25
	CO	12.90	20.99
	CO$_2$	75.00	206.13
	CH$_4$	10.50	8.64
0.5% Mn/Al$_2$O$_3$	VOCs	82.40	14.04
	Benzene	78.78	5.73
	Toluene	83.85	4.40
	Xylene	85.71	3.90
	CO	16.70	24.08
	CO$_2$	76.00	172.03
	CH$_4$	11.00	8.99
1% Mn/Al$_2$O$_3$	VOCs	78.10	28.04
	Benzene	73.57	12.35
	Toluene	74.33	9.08
	Xylene	79.70	6.61
	CO	25.80	41.83
	CO$_2$	62.00	148.27
	CH$_4$	11.50	10.48
2% Mn/Al$_2$O$_3$	VOCs	71.80	20.82
	Benzene	61.63	11.09
	Toluene	77.91	6.20
	Xylene	88.03	3.53
	CO	19.80	22.10
	CO$_2$	63.00	158.66
	CH$_4$	11.50	8.70
3% Mn/Al$_2$O$_3$	VOCs	80.90	16.87
	Benzene	75.07	6.93
	Toluene	77.84	6.27
	Xylene	86.95	3.67
	CO	16.10	18.45
	CO$_2$	70.50	162.33
	CH$_4$	10.50	9.23

Catalyst	Parameters	Conversion /Selectivity (%)	Outlet Concentration (ppm)
4% Mn/Al$_2$O$_3$	VOCs	84.40	15.78
	Benzene	77.75	7.17
	Toluene	84.90	4.91
	Xylene	88.46	3.70
	CO	15.50	20.96
	CO$_2$	71.00	186.94
	CH$_4$	9.50	9.63
5% Mn/Al$_2$O$_3$	VOCs	95.00	4.17
	Benzene	92.84	1.95
	Toluene	95.32	1.37
	Xylene	97.16	0.84
	CO	14.70	27.16
	CO$_2$	77.00	211.83
	CH$_4$	9.00	8.88